ELECTRON MICROSCOPE STUDY OF THE MICROSTRUCTURE OF BIS 812 EMA SUBMARINE STEEL

AR-006-828

AD-A267 044

MATERIALS RESEARCH LABORATORY
DSTO

Electron Microscope Study of the Microstructure of BIS 812 EMA Submarine Hull Steel

I.M. Robertson

MRL Technical Report
MRL-TR-91-35

Abstract

The hull steel for Australia's Collins class submarine, BIS 812 EMA, is somewhat unusual in that it contains significant additions of boron and the substitutional hardenability elements nickel, chromium and molybdenum, and is also microalloyed with titanium, niobium and vanadium. It is used in the quenched and tempered condition, rather than being control-rolled, and therefore the role and benefit conferred by the microalloying additions are not clear. The electron microscope study reported here is concerned with characterizing the microstructure of the steel and determining the distribution of the titanium, niobium and vanadium.

The steel consists of tempered lath martensite typical of quenched and tempered steels of similar carbon content. The titanium occurs as cuboidal particles, ten to one hundred nanometres in size (probably TiN), formed after solidification or during the soak, and largely unaffected by subsequent processing. The niobium and vanadium appear to be mostly taken into solution during the austenitizing treatment and precipitate as a fine carbide dispersion during tempering, although some niobium is incorporated in the "TiN" cuboids.

DSTO MATERIALS RESEARCH LABORATORY

Published by

Materials Research Laboratory
Cordite Avenue, Maribyrnong
Victoria, 3032 Australia

Telephone: (03) 246 8111
Fax: (03) 246 8999

AR No. 006-828

APPROVED FOR PUBLIC RELEASE

Author

I.M. Robertson

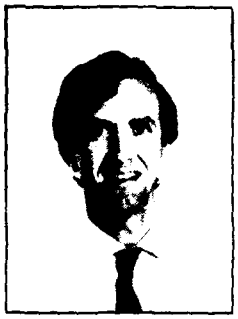

Dr Ian Robertson served as a metallurgist at the Commonwealth Steel Company and graduated BMet (Hons) from the University of Newcastle in 1979. He was awarded a PhD in Metallurgical Engineering from the University of Illinois in 1983 for research on electron microscopy of shape memory alloys. He returned to Australia as an AINSE research fellow at the University of Newcastle, carrying out neutron diffraction work at Lucas Heights. After four years at the Comalco Research Centre engaged in research on rolled aluminium alloys, he joined MRL in 1988. At MRL his main interests have been magnetic properties of ferromagnetic materials, and fatigue of welded structures. He has broad experience in ferrous and non-ferrous metallurgy, and modern techniques for materials characterisation.

Contents

Electron Microscope Study of the Microstructure of BIS 812 EMA Submarine Hull Steel

1. Introduction

BIS 812 EMA steel produced in Australia for the pressure hull of the Collins class submarine is based on OX 812 EM steel developed in Sweden by SSAB (Stark, 1987). It is similar to ASTM grade A 514 Class F (ASM, 1978) and bears some resemblance to the well known T1 steel developed by US Steel. In common with other submarine steels, it is designed to have a combination of high strength and toughness together with good weldability.

In the current investigation, the steel was examined using optical, scanning electron and transmission electron microscopy to determine its microstructure. Emphasis was given to the distribution and form of the titanium, niobium and vanadium microalloying additions. It was not clear whether these elements are strictly necessary to obtain the mechanical properties required of BIS 812 EMA steel in the quenched and tempered condition.

The composition of the sample used in the study is listed in Table 1. Some points to note are as follows:

(i) The phosphorus and sulphur levels are very low in order to minimise the number of non-metallic inclusions and allow the required toughness to be achieved (Pickering, 1977; Lubuska, 1977).

(ii) Additions of nickel, chromium and molybdenum are made to confer hardenability (Bain and Paxton, 1966). Nickel also improves low temperature toughness.

(iii) Boron is added for additional hardenability at a concentration typical of boron-treated alloy steels (see Appendix 1).

(iv) The steel is aluminium killed and also has a titanium addition to protect the boron from nitrogen (Croll, 1984; Killmore, Harris and Williams, 1984). Aluminium is itself required to protect the titanium from forming TiO_2 (Sellars and Beynon, 1984). Titanium binds the nitrogen in the steel as TiN particles formed at high temperature (Roberts, 1984).

(v) In addition to titanium, there are significant microalloying additions of niobium and vanadium. The latter contribute to hardenability, but are more important because they often precipitate as carbo-nitride particles in steels. They can have a profound influence on the recrystallisation, transformation and tempering processes in steels (e.g. Pickering, 1984).

(vi) The steel is calcium treated for inclusion shape control and improved toughness (Wilson, 1984).

Table 1: *Chemical Composition of BIS 812 EMA Sample*

Alloying Element	Weight Percent		Atomic Percent
	Heat Analysis (Heat 8337316)	Sample Analysis	
C	0.14	0.14	0.65
Si	0.27	0.25	-
Mn	0.98	0.91	-
P	0.010	0.010	-
S	0.001	0.002	-
Ni	1.30	1.26	-
Cr	0.52	0.45	-
Mo	0.37	0.38	-
Cu	0.21	0.19	-
Ti	0.006	0.01	0.007
Nb	0.010	0.01	0.006
V	0.022	0.02	0.024
B	0.0025	0.0044	0.02
Al	0.075	0.095	0.18
N	0.0072	0.006	0.024

Processing of BIS 812 EMA consists of basic oxygen steelmaking, secondary ladle treatment, continuous casting to slabs about 220 mm thick, soaking at about 1200°C and hot rolling to the required plate thickness. This is followed by austenitizing at about 900°C, quenching, and tempering at about 650°C to achieve a minimum yield strength of 690 MPa.

2. *Materials and Methods*

The steel used in the study was a sample from normal production plate cast (Heat number 8337316) and rolled by BHP Steel International (Slab and Plate Products Division, Pt. Kembla). The basic processing route has been described by Killmore et al. (1984). The plate was quenched and tempered by Bisalloy Industrial Steels (Unanderra) using roller quench equipment described by Croll (1984). The composition is listed in Table 1. Hardness is constant through the plate thickness at about 263 HV (equivalent to about 880 MPa ultimate tensile strength).

Specimens were prepared from the plate in its as-received condition. Additional specimens were obtained after further heat treatment at MRL, including a water quench after 15 minutes in a salt bath maintained at 915°C and subsequent tempering (to reproduce the microstructure development during the original quench and temper treatment). The austenitizing time is sufficient for homogenisation of steel which has previously been quenched and tempered.

Three types of specimen were prepared for examination using optical, scanning electron and transmission electron microscopy. All specimens were oriented perpendicular to the plate rolling direction. The preparation procedures were as follows:

(i) Optical microscopy specimens were mounted, ground and polished using standard metallographic techniques. The specimens were examined unetched to determine the size and distribution of non-metallic inclusions. The same specimens were examined using a Cambridge Instruments Stereoscan 250 Mk II scanning electron microscope (SEM) fitted with a Link Analytical AN 10/85 S energy dispersive X-ray analysis system (EDS).

(ii) Carbon extraction replicas for transmission electron microscopy (TEM) were prepared from the optical microscopy specimens. The specimens were lightly etched in Vilella's reagent (three seconds) and carbon evaporation coated. After scoring the carbon coating into 2 mm grid squares, the squares were stripped by etching in Vilella's reagent and floated onto distilled water. The squares were transferred through several washes of distilled water before mounting on 3 mm diameter copper support grids.

(iii) Thin foils for TEM were prepared by traditional methods. This consisted of electro-discharge machining a thin slice from the sample, grinding and chemical polishing (hydrogen peroxide/phosphoric acid solution) to a thickness of 70 μm, punching out 3 mm diameter discs, dimpling in a Struers Tenupol twin jet electro-polishing unit (10% perchloric acid, 70% ethanol, 20% glycerol electrolyte), and final electro-polishing at 35 V using a chromic acid/acetic acid/water electrolyte.

The TEM specimens were examined using a Philips EM 301 microscope operated at 80 kV for most of the investigation. Supplementary micro-analysis was carried out using a JEOL 2000 FX STEM fitted with a Tracor Northern 5500 energy dispersive X-ray analysis system.

3. *Results*

3.1 Optical and Scanning Electron Microscopy

The main interest for this part of the investigation was in the coarse non-metallic inclusions in the steel. Such inclusions are up to several microns in size and are formed in the melt or soon after solidification. The three types identifiable by optical microscopy in BIS 812 EMA steel are as follows:

(i) Grey, slightly elongated sulphide inclusions.
(ii) Black, globular oxide inclusions.
(iii) Orange-pink faceted inclusions.

The sulphide and oxide inclusions are the most common types. The coloured, faceted inclusions are less numerous.

Analysis of the inclusions using EDS revealed that:

(i) The sulphide inclusions are for the most part the usual MnS, but occasionally also contain a small amount of titanium.

(ii) The oxide inclusions contain the expected aluminium and silicon.

(iii) The coloured inclusions usually contain titanium and a lesser amount of niobium. This identifies them as carbo-nitrides. Similar inclusions were observed by Chen, Loretto and Cochrane (1987) in Ti-Nb-V and Ti-Nb steels (but not in a Nb-V steel). They determined that the inclusions are basically TiN with the outer layers enriched in Nb(C,N). The inclusions result from segregation and are detrimental to mechanical properties.

Vanadium also forms carbo-nitride, but EDS spectra did not clearly reveal its presence in the coarse inclusions visible in the optical microscope. However, it should be noted that vanadium K X-rays fluoresce titanium, leading to low vanadium X-ray peak intensity in the presence of titanium (Lehtinen and Hansson, 1989).

The presence of titanium in sulphide inclusions and its dominance over niobium and vanadium in the coarse carbo-nitrides is in accord with previously published findings. More detail is given in Appendix 2.

An optical micrograph showing the basic tempered martensite structure of the steel and some EDS spectra from the common non-metallic inclusions are presented in Figures 1 and 2 respectively.

Typical SEM micrographs of the carbo-nitride inclusions are shown in Figure 3, together with EDS analysis spectra in Figure 4. The dark inclusions in the back-scattered electron images have a high titanium concentration and a lesser amount of niobium. The niobium-rich inclusion (Figure 3b, 4b) appears light-coloured because of the high atomic weight of niobium.

3.2 *Transmission Electron Microscopy*

The microstructure of the steel in the as-received (quenched and tempered) condition consists of recovered lath martensite, with carbides precipitated within the laths and on the lath boundaries during tempering. The microstructure is therefore similar to that reported for other carbon and alloy steels of similar carbon content (For reviews see Honeycombe, 1981, and Petty, 1970. The basic processes occurring during tempering are summarised in Appendix 3).

Various aspects of the microstructure are considered in the following sections. One type of cementite (Fe_3C) particle is found in coarse martensite laths formed in the early stages of the martensitic transformation (during the quench). A different type forms, during tempering, on the boundaries of finer laths formed at later stages of the martensitic transformation. Cuboidal TiN precipitates inherited from the austenite were also found.

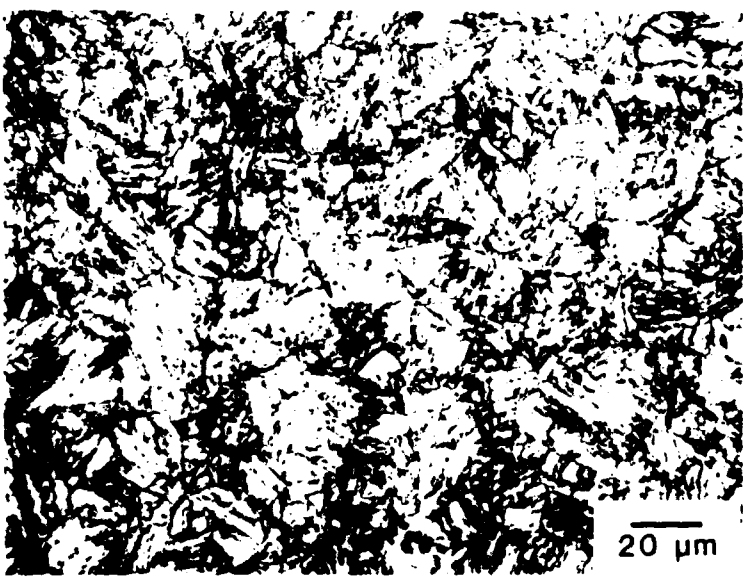

Figure 1: *Optical micrograph of BIS 812 EMA microstructure (Etchant: 2% nital).*

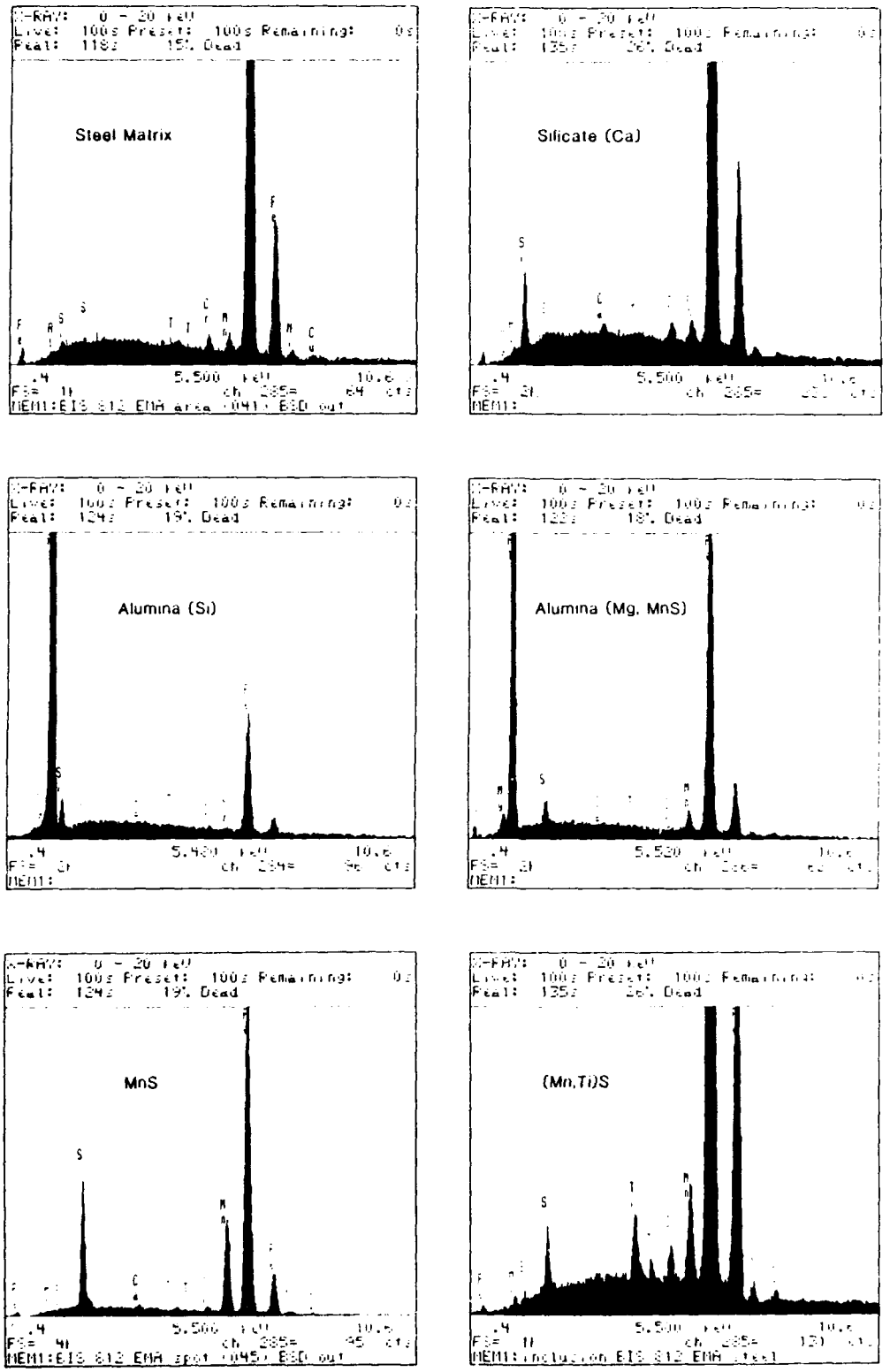

Figure 2: EDS spectra from non-metallic inclusions in BIS 812 EMA.

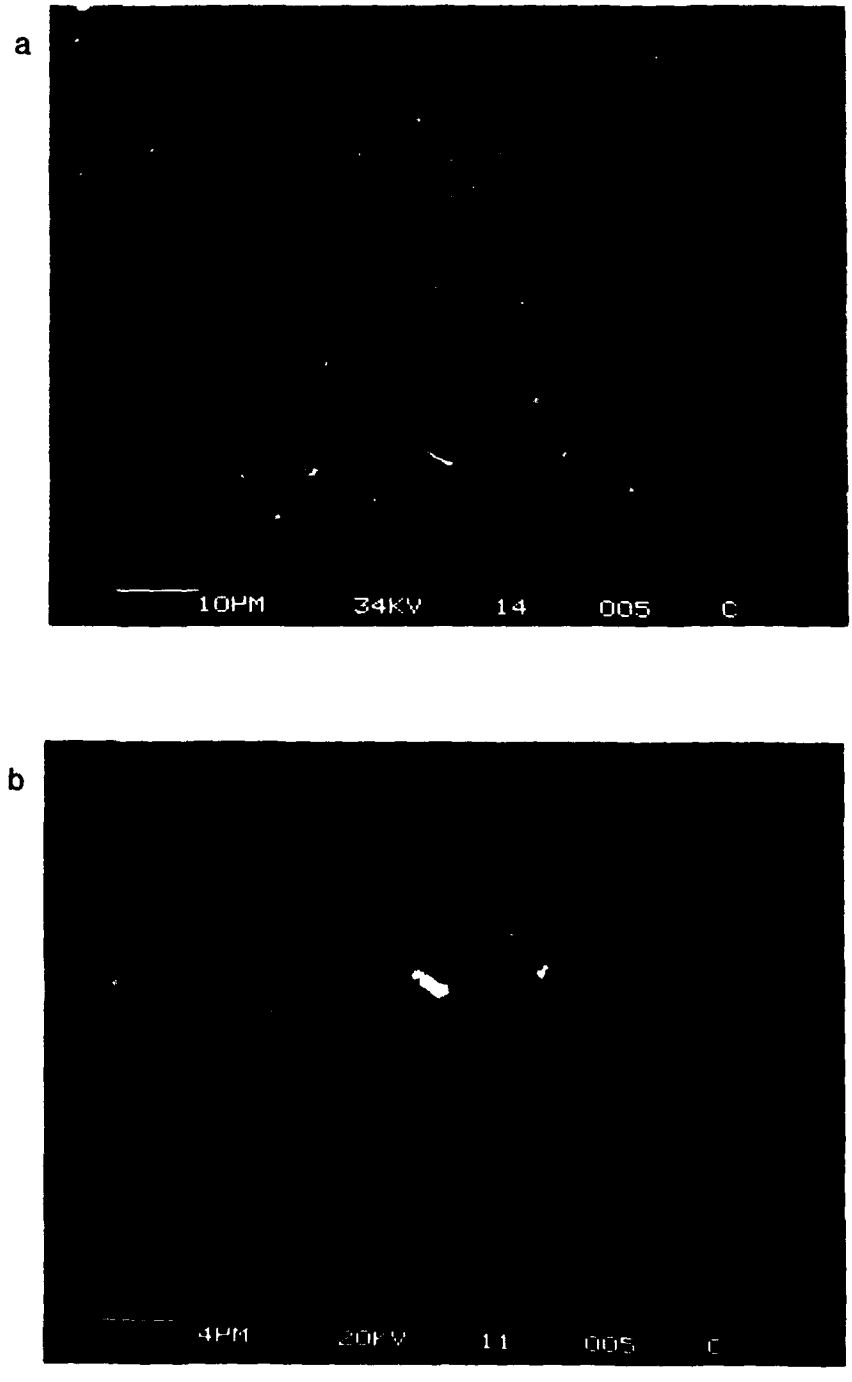

Figure 3: *Scanning electron micrographs (backscatter image) of coarse alloy carbonitrides in as-received BIS 812 EMA stee..*

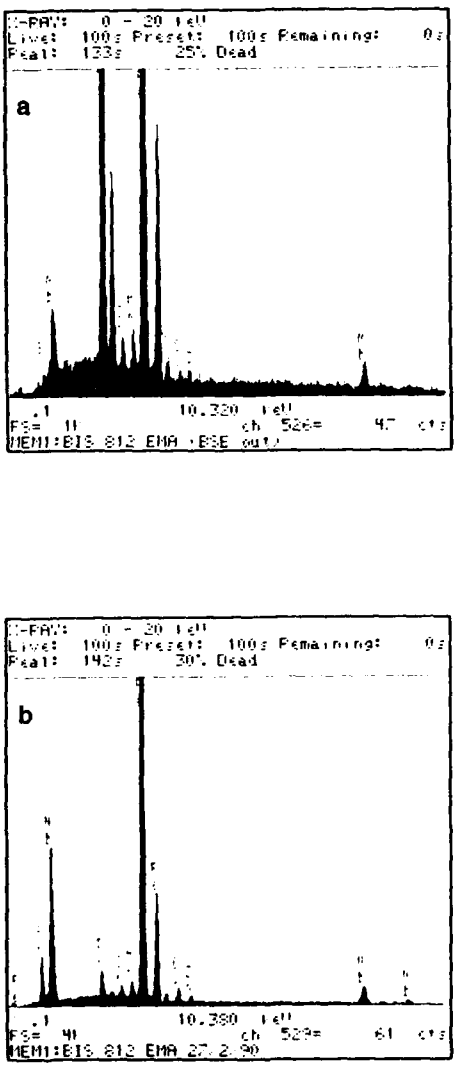

Figure 4: *Energy dispersive X-ray analysis spectra of the coarse carbo-nitrides in Figure 3. (a) Analysis of largest particle in Figure 3a showing a large concentration of Ti, some Nb and possibly a small amount of V, in addition to Fe, Cr, Mn and Ni from the matrix. (b) Analysis of small white particle adjacent to larger arrowhead particle in Figure 3b showing a large amount of Nb and some Ti (Si, Cu and Zn from BSE detector).*

3.2.1 *Tempered Lath Martensite*

The distribution of temper carbides and other particles in as-received BIS 812 EMA is shown in Figure 5 (low magnification micrographs of extraction replicas). Most of the carbides are essentially cementite (Honeycombe, 1981; Petty, 1970) but they have two different morphologies as follows:

(i) Globular particles, apparently distributed fairly randomly in the structure (thin foil micrographs show more detail, see below).
(ii) Widmanstatten rod- or plate-shaped particles restricted to a small number of crystallographic habit planes.

EDS analysis of both types of particle in an extraction replica revealed the presence of mainly iron together with some Cr, Mn, Ni and Mo (and occasionally Si). EDS does not detect light elements such as carbon.

The thin foil micrographs of Figures 6 and 7 reveal the typical (recovered) lath martensite structure. In Figure 6 the laths lie in the plane of the foil, whereas in Figure 7 they are in a more end-on orientation. The same figures also reveal that the globular particles of Figure 5 are not randomly distributed but are usually located on the martensite lath boundaries (a preferred site for precipitation during tempering). They have aspect ratios of up to about 3:1.

In addition to the fine lath structure of Figures 6 and 7, coarser laths are present in the structure. It is these laths which contain the Widmanstatten precipitates. Figure 8 shows such a lath adjacent to a prior austenite grain boundary. The presence of the Widmanstatten precipitates is attributed (e.g. Law, Howell and Edmonds, 1979) to autotempering of the first laths to form during martensitic transformation. Cementite precipitates which form by autotempering are known to form as laths on the {110} planes of ferrite (Appendix 3, Tekin and Kelly, 1965).

3.2.2 *As-Quenched Structure*

Specimens were prepared from a sample water quenched from 915°C at MRL (not tempered) in order to check for the presence of autotemper cementite. In addition to delineating prior austenite grain boundaries and the martensite lath structure, extraction replicas indeed reveal the presence of Widmanstatten carbides within coarse as-quenched laths. These are apparent in the micrographs of Figure 9 but are more clearly revealed in the higher magnification, thin foil micrographs of Figure 10. Globular temper carbides are not present.

Extraction replicas of the Widmanstatten carbides in as-quenched and as-received (tempered) specimens are compared in Figure 11 (at higher magnification than in Figures 5 and 9). The carbide particles are more efficiently extracted after tempering, probably because tempering causes them to thicken and become more globular. As quenched they are very thin plates or laths. For plain carbon steels, the Widmanstatten cementite precipitates do not persist on tempering above about 350°C but in alloy steels (containing Cr, Mo and V) they are stable to much higher tempering temperatures.

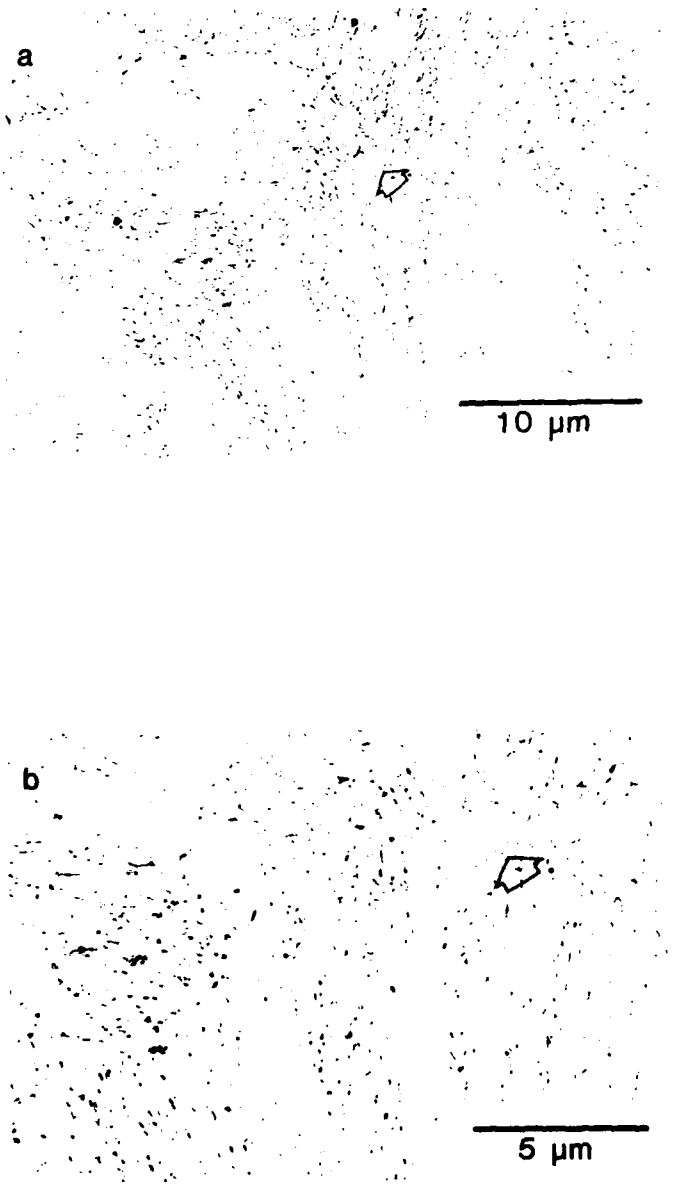

Figure 5: TEM micrographs of carbon extraction replica from as-received BIS 812 EMA steel. The black spots are carbide particles extracted from the steel. Arrow indicates an area of crystallographically oriented particles.

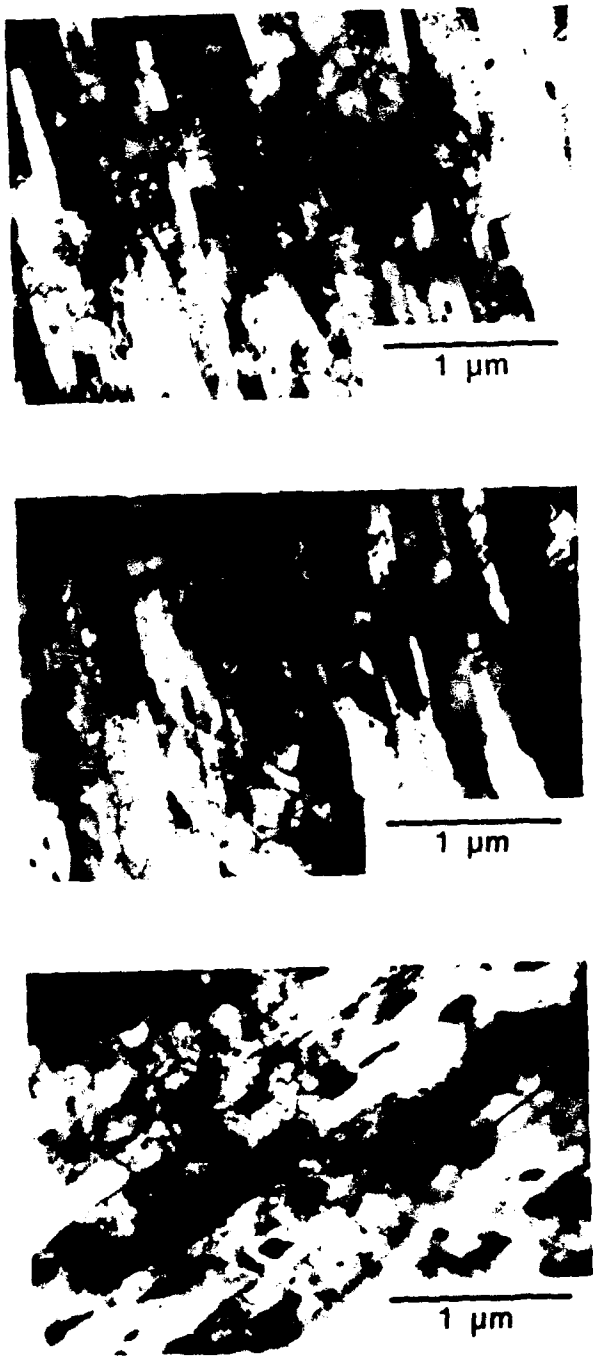

Figure 6: TEM thin foil micrographs from as-received BIS 812 EMA showing martensite laths in the plane of the foil. Different areas of the foil show different densities of cementite precipitates.

Figure 7: TEM thin foil micrograph of as-received BIS 812 EMA showing martensite laths out of the plane of the foil.

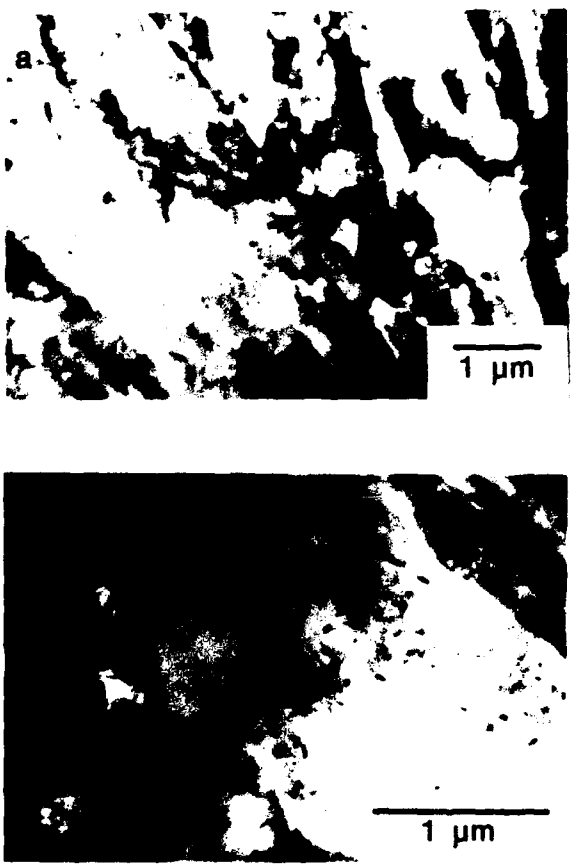

Figure 8: TEM thin foil micrographs of as-received BIS 812 EMA. A prior austenite grain boundary (arrowed) separates a region of fine martensite laths and a coarse lath. The coarse lath contains Widmanstatten carbides (typical length 0.1 μm).

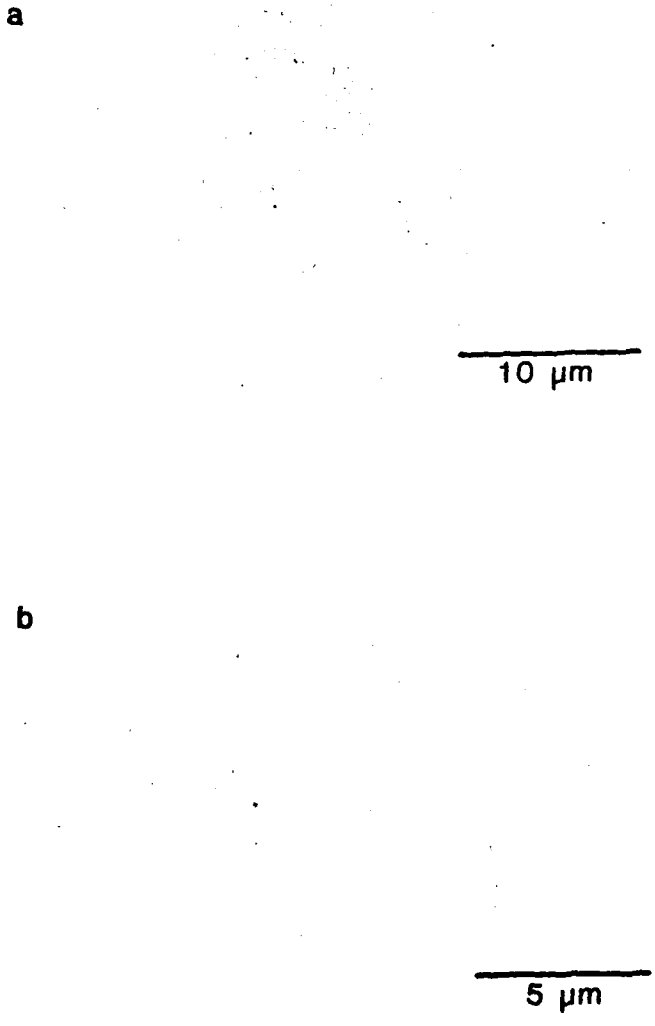

Figure 9: TEM micrographs of a carbon extraction replica from as-quenched BIS 812 EMA, showing prior austenite grain boundaries, martensite lath structure and Widmanstatten (autotemper) carbides. See also Figures 10 and 11.

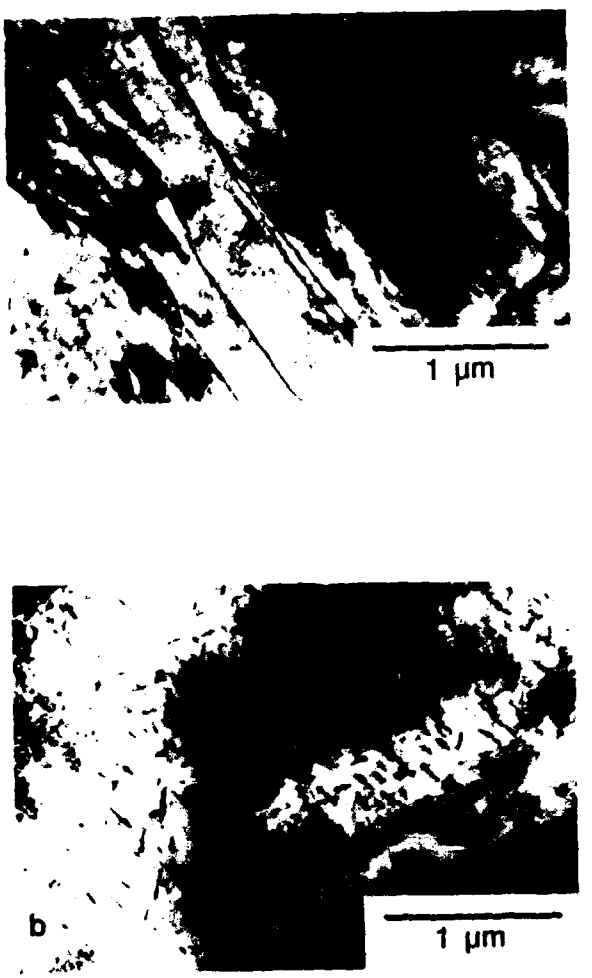

Figure 10: *TEM thin foil micrographs of as-quenched BIS 812 EMA showing (a) martensite lath structure, (b) Widmanstatten carbides in a coarse lath (typical length 0.12 µm).*

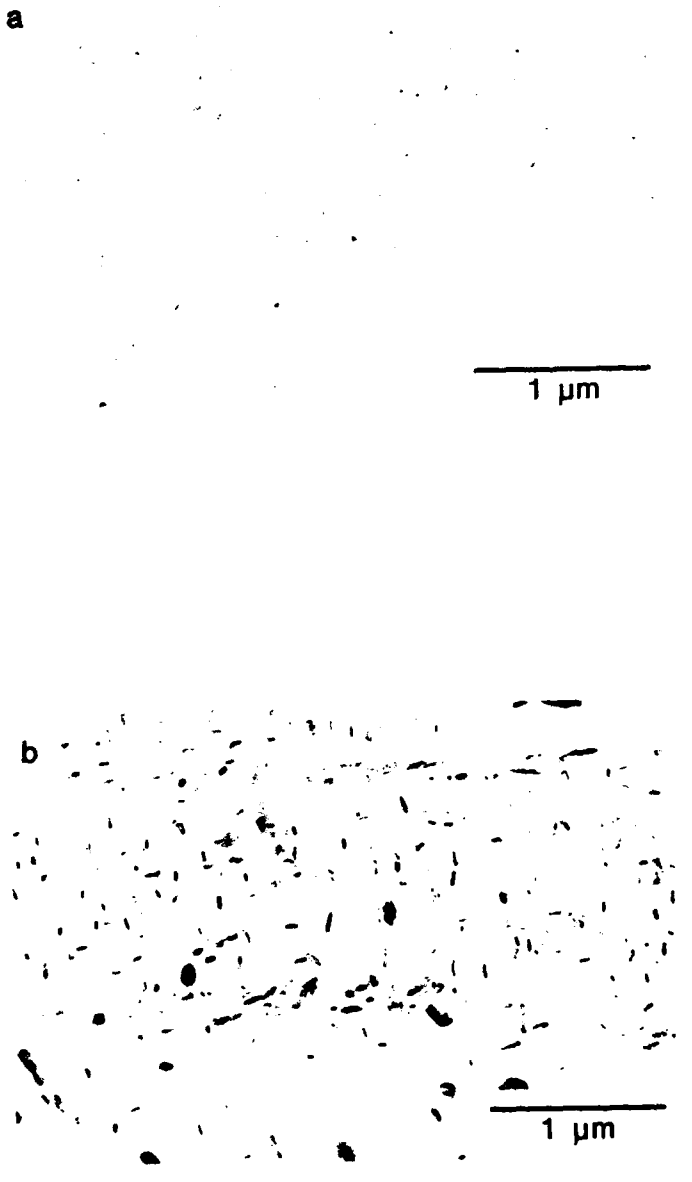

Figure 11: *TEM micrographs of carbon extraction replicas from BIS 812 EMA in (a) as-quenched, and (b) as-received conditions. Widmanstatten carbides and fine TiN cuboids are visible in (a). Widmanstatten and some globular carbides are visible in (b).*

3.2.3 *Alloy Carbo-Nitrides*

The cementite precipitates referred to in Sections 3.2.1 and 3.2.2 are similar to those found in unalloyed steels. EDS analysis spectra taken from these particles were essentially the same as those from the steel matrix. It is known that vanadium has some solubility in cementite (Pickering, 1984) but no vanadium was detected in any of the particles analysed.

In addition to the cementite particles, a fine dispersion of cuboidal precipitates was also found in the steel, in both the as-received and as-quenched conditions. The particles were apparently unaffected by the austenitizing treatment at 915°C, indicating low solubility at this temperature. Some of the particles are shown in Figure 12 (as-quenched replica) and Figure 13 (as-received replica).

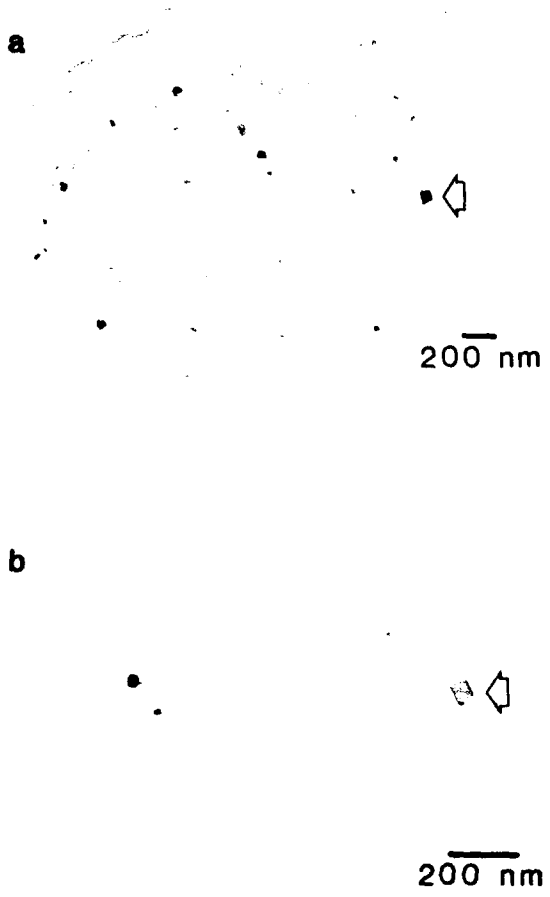

Figure 12: *High magnification TEM micrographs of a carbon extraction replica from as-quenched BIS 812 EMA showing TiN cuboids. The micrographs were taken from an area containing a high density of particles.*

Figure 13: *As for Figure 12 but as-received replica. Temper carbides are present in addition to the TiN cuboid arrowed.*

EDS analysis showed that the particles contain titanium, usually but not always together with niobium (Figure 14). They are probably TiN formed during cooling after casting, with the outer layers enriched in niobium due to subsequent growth at lower temperature (See Section 4 on the precipitation of mixed alloy carbo-nitrides). Such TiN particles are frequently observed in titanium-treated steels (See Appendix 2). The size distribution depends on the cooling rate after solidification (Roberts, 1984). For BIS 812 EMA, the TiN precipitates range in size from about 10 nm to about 100 nm, with most in the range 20 to 50 nm. A similar size distribution has been reported by Feng, Chandra and Dunne (1989) for a steel of similar composition produced at the same steel mill. As far as qualitative EDS analysis permits, the composition of the cuboids is very similar to that of the coarse, coloured inclusions observed using optical microscopy and SEM (Section 3.1).

3.2.4 Distribution of Niobium and Vanadium

The observations reported above account for the titanium microalloy addition and part of the niobium. However the vanadium and remaining niobium were more elusive. It is possible that these elements remain in solid solution in the steel matrix, but it is more probable that they occur as finely dispersed precipitates on a scale difficult to detect using even TEM.

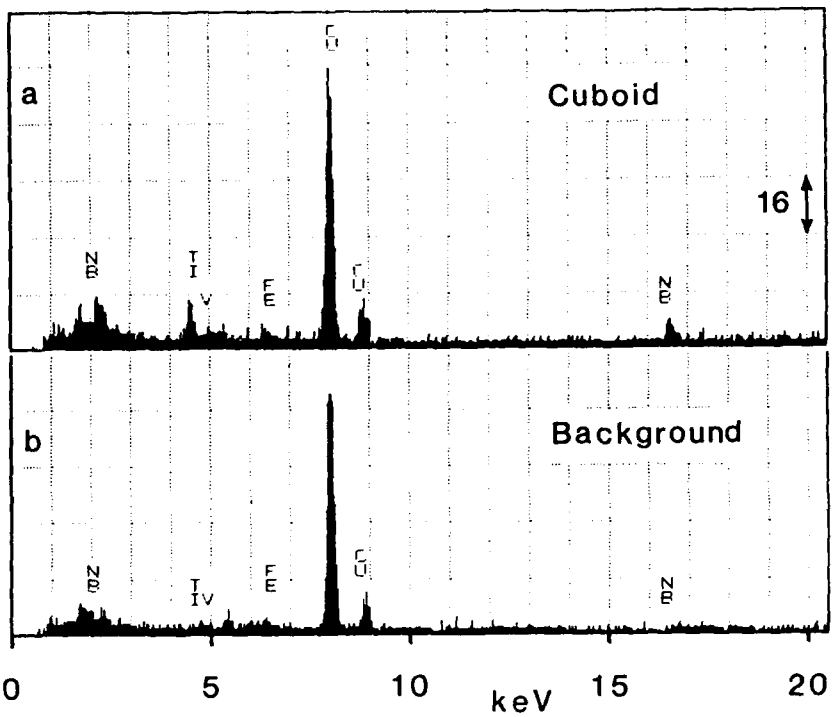

Figure 14: EDS spectra from "TiN" cuboids in a replica from as-quenched BIS 812 EMA. Similar spectra were obtained from cuboids in an as-received BIS 812 EMA thin foil. The Cu peaks originate from the replica support grid. (a) Cuboid spectrum showing Ti, Nb and possibly Fe peaks. (b) Background spectrum.

A survey of the literature (see references in Table 2) indicates that most of the vanadium and some of the niobium in BIS 812 EMA should be soluble (at equilibrium) in austenite at the austenitizing temperature of 900°C. The remaining niobium would precipitate on a fine scale within the austenite grains and on austenite grain and sub-grain boundaries during hot rolling or during the austenitizing treatment (For more detail on niobium precipitation in austenite see Appendix 4). On tempering, both niobium and vanadium are expected to precipitate (as carbide or carbo-nitride) on matrix dislocations on a very fine scale (Appendix 3).

Examination of replicas from as-quenched BIS 812 EMA revealed some very fine (< 5 nm) particles which could contain niobium, but these are just as likely to be TiN precipitates. Figures 15 and 16 show the results of attempts to image any fine scale VC or Nb(C,N) precipitation in as-received BIS 812 EMA using bright field and dark field imaging respectively. There is some indication of precipitation on dislocations, but the results are at best equivocal because of the oscillating "dot" contrast on inclined dislocations even in the absence of precipitation. Most studies of steels exhibiting this type of precipitation have involved much greater microalloy additions and/or tempering times, so it is not surprising that clear evidence of fine scale precipitation on dislocations was not obtained in the present case.

Table 2: Solubility in Austenite

Metal, M	$\log_{10}$ [%M] [%N]	$\log_{10}$ [%M] [%C]
B	5.24 – 13970/T	
Al	1.03 – 6770/T	
	1.95 – 7400/T	
	1.79 – 7184/T	
	0.725 – 6180/T	
	1.8 – 7750/T	
	1.48 – 7500/T	
Ti	3.9 – 15200/T	2.75 – 7000/T
	3.82 – 15020/T	5.33 – 10475/T
	6.75 – 19740/T	
	0.322 – 8000/T	
	5.0 – 14400/T	
Nb	2.80 – 8500/T	2.26 – 6770/T
	4.96 – 12230/T	3.42 – 7900/T
	3.70 – 10800/T	3.11 – 7530/T
	4.04 – 10230/T	3.3 – 7900/T
		3.04 – 7290/T
		4.37 – 9290/T
		(-0.63 – 250/T)
		(3.7 – 9100/T)
		(5.43 – 10960/T)
V	3.46 – 8330/T	6.72 – 9500/T
	3.63 – 8700/T	
	2.99 – 7733/T	
	3.02 – 7840/T	
	2.27 – 7070/T	
Zr		4.26 – 8464/T

VN:	$\log[V][N]$	=	3.46 + 0.12[Mn] - 8330/T
V_4C_3	$\log[V]^{4/3}[C]$	=	7.06 - 10800/T
	$\log[V][C]^{3/4}$	=	5.36 - 8000/T
NbC:	$\log[Nb][C]$	=	3.31 + 0.27[Mn] - 0.28[Si] + 0.04[Ni] + 0.26[Cr] -7970/T
$NbC_{0.87}$	$\log[Nb][C]^{0.87}$	=	3.18 - 7700/T
Nb(C,N):	$\log[Nb][C+N]$	=	1.54 - 5860/T
	$\log[Nb][C+12N/14]$	=	2.26 - 6770/T
	$\log[Nb][C]^{0.83}[N]^{0.14}$	=	4.46 - 9800/T
	$\log[Nb][C]^{0.24}[N]^{0.65}$	=	4.09 - 10400/T

Temperature, T, is in Kelvin.
Composition, [ ], is in weight percent.
Expressions in brackets ( ) give solubilities much higher or lower than the other expressions.

References:

Ashby and Easterling (1982)
Hoogendorn and Spanraft (1977)
Kampshaefer and Jesseman (1977)
Koyama et al. (1971)
Leslie (1981)
Matsuda and Okumura (1978)
McLean and Kay (1977)
Speer et al. (1987)
Strid and Easterling (1985).

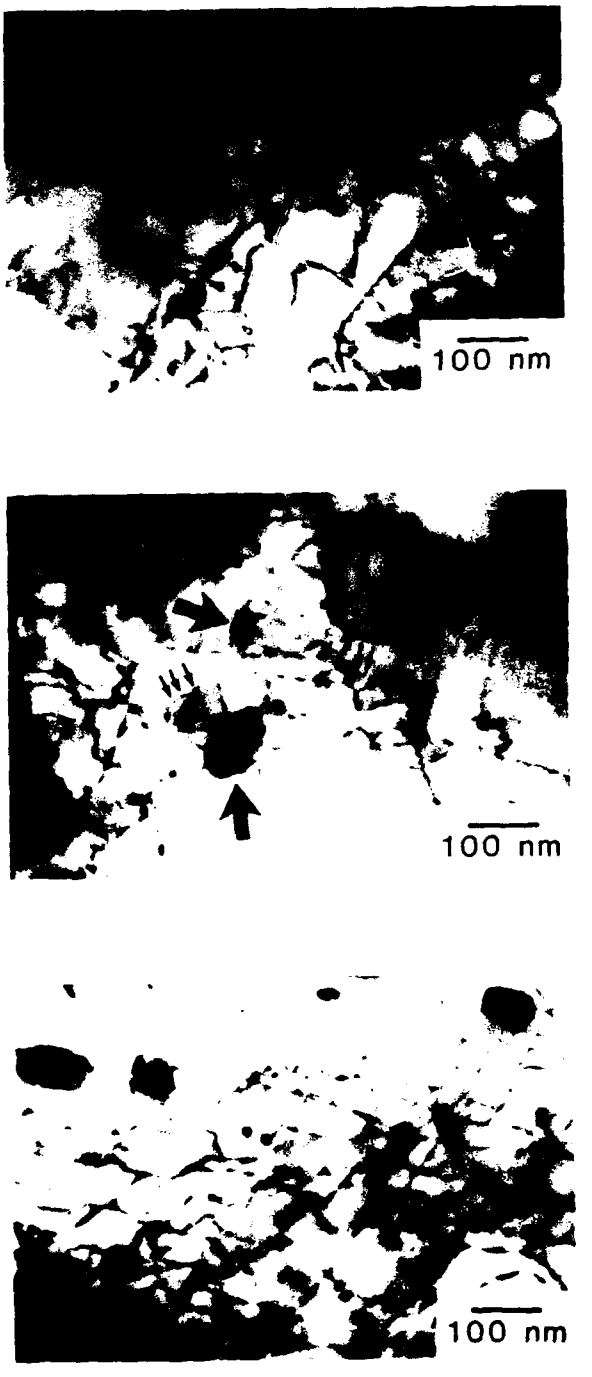

Figure 15: *TEM thin foil micrographs of dislocations in as-received BIS 812 EMA. Coarse globular cementite particles (heavy arrows) are clearly shown but the evidence for fine alloy carbonitride precipitates on dislocations (light arrows) is not strong.*

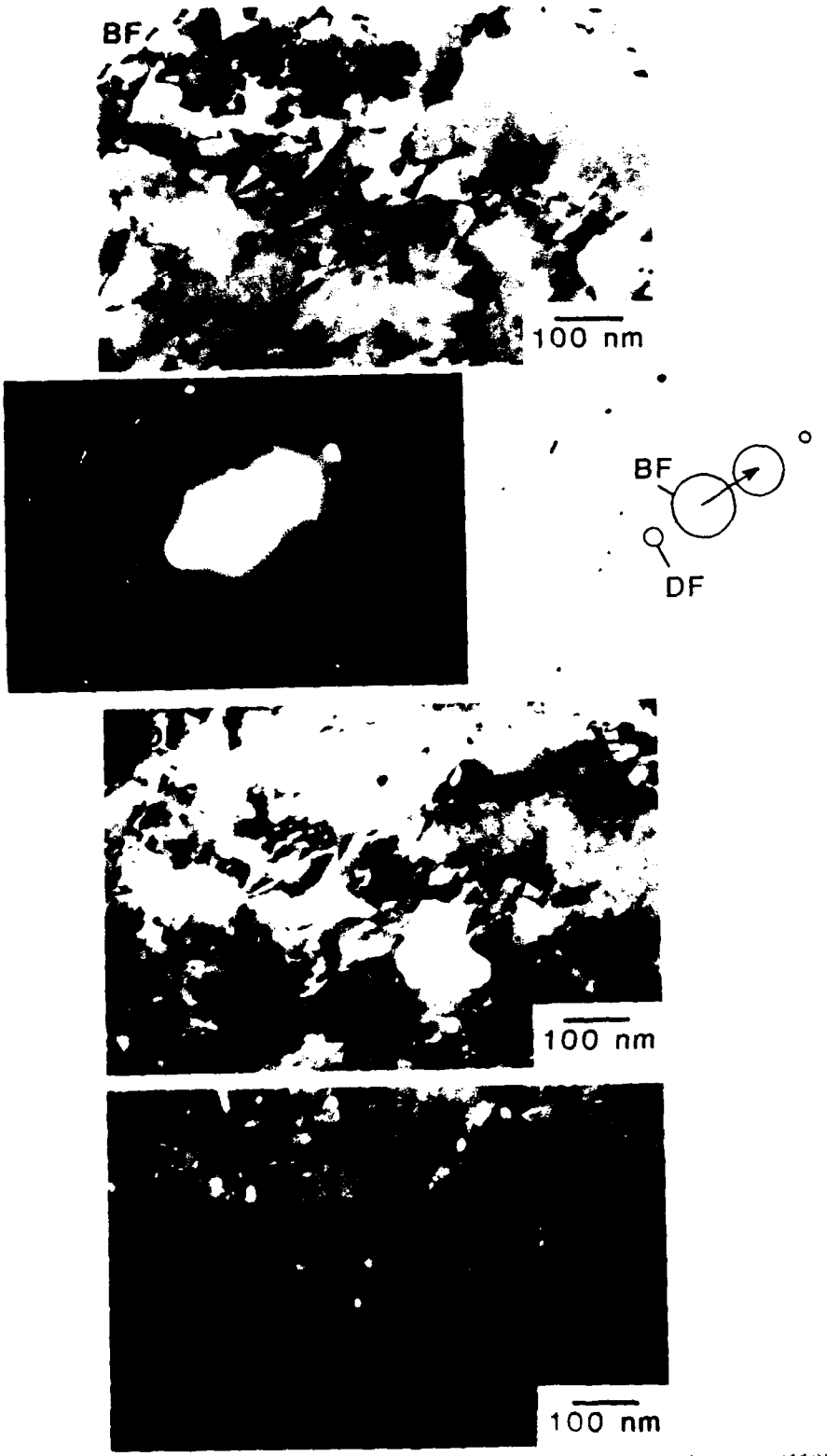

Figure 16: *Bright field, dark field and weak beam dark field images, using a g = (110) reflection, of the same area of a thin foil of as-received BIS 812 EMA. The diffraction pattern corresponding to the bright field image is also shown.*

In order to clarify the situation, the tempering resistance of BIS 812 EMA was compared with that of three laboratory heats of similar composition. One of the laboratory heats (produced by BHP-MRL) contained titanium, niobium and vanadium as for BIS 812 EMA, one contained titanium and vanadium, and the third contained only titanium. After quenching the steels from 915°C the hardness of the four specimens was measured during tempering. It is known that niobium and vanadium in solution at the austenitizing temperature contribute to secondary hardening and retardation of tempering due to precipitation of carbo-nitrides during the temper. This "secondary hardening potential" has been used as a measure of the amount of alloying element remaining in solution in austenite (e.g. Crowther, Mohamed and Mintz, 1987).

It was found in the present study that the loss of hardness after tempering for four hours at 600°C (compared with the as-quenched hardness) gave good differentiation between the steels. The results are as follows:

Ti (no Nb, V)	Loss of 171 Vickers hardness points
Ti, V (no Nb)	Loss of 136 Vickers hardness points
Ti, Nb, V	Loss of 125 Vickers hardness points
BIS 812 EMA	Loss of 120 Vickers hardness points

The results are in good qualitative agreement with the temper resistance expected from the solubility of vanadium and niobium in BIS 812 EMA. The vanadium (all 0.025% expected to be in solution at the austenitizing temperature) accounts for about 35 HV of temper resistance. The niobium (about half, 0.005%, expected to be in solution) provides another 10 to 15 HV of temper resistance. According to Lin and Hendrickson (1988), niobium is about 2.5 times as effective as vanadium as a precipitation hardener.

In summary, it is apparent that most of the vanadium and about half the niobium in BIS 812 EMA remain in solution in austenite before quenching. During tempering they precipitate on a very fine scale (too fine to be observed using TEM) causing a significant retardation in the loss of hardness due to tempering.

4. *Discussion*

The basic aim of the current investigation was to determine the role of the microalloying additions titanium, niobium and vanadium. TEM observations have been successful in locating the titanium and at least some of the niobium, and have provided equivocal evidence of additional fine scale precipitation of niobium and vanadium. However, hardness measurements during tempering indicate that both niobium and vanadium are in solution during austenitizing and precipitate during tempering. In this section the behaviour of titanium, niobium and vanadium is examined from a more theoretical viewpoint, beginning with their solubility in austenite.

The solubility of alloy carbo-nitrides in austenite has been investigated in numerous studies because of the importance of carbo-nitride precipitates to the processing of HSLA steels. A compilation of expressions for solubility products as a function of temperature is listed in Table 2. These relations are plotted in Figures 17 and 18 for temperatures of 1200°C and 900°C (the austenitizing temperature) respectively.

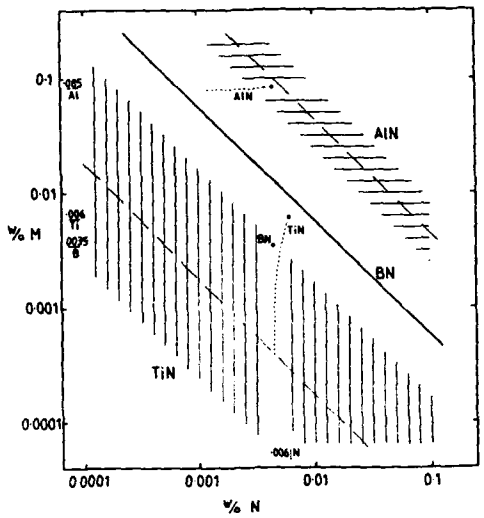

Figure 17: Solubility limits for various phases in austenite at 1200°C from the expressions shown in Table 2. Curves are also shown for the change in composition of the austenite due to precipitation of stoichiometric TiN, followed by precipitation of AlN, using the composition of the BIS 812 EMA sample as the starting composition.

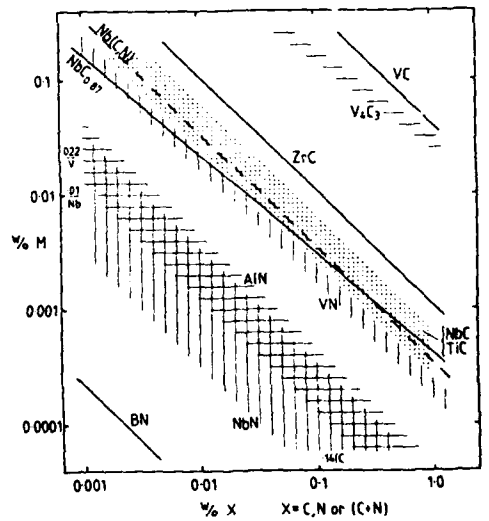

Figure 18: As for Figure 17 but for a temperature of 900°C. The expressions for NbC in brackets in Table 2 have not been plotted because they are not in good agreement with the other results. The solubilities of NbC and TiC are very similar, and have been shown as a single uncertainty band. The solubility of TiN is off scale at the lower left hand corner.

Figures 17 and 18 illustrate the very low solubility of TiN compared with other nitrides, especially when it is noted that NbN is found only in very low carbon steels (Strid and Easterling, 1985) and niobium usually occurs as Nb(C,N). Therefore TiN is the first phase to precipitate, and removes titanium and nitrogen from solution in the stoichiometric proportion (Sellars and Beynon, 1984). For the composition of BIS 812 EMA, Figure 17 shows that TiN is the only phase to have exceeded its solubility by the time the steel has cooled to 1200°C (At this temperature AlN is near to its solubility limit assuming 0.085% soluble aluminium). Using three pieces of information:

(i) The titanium content of 0.006% and nitrogen content of 0.006%
(ii) Removal of titanium and nitrogen as stoichiometric TiN,
(iii) The solubility limit at 1200°C (Figure 17),

the distribution of titanium and nitrogen are calculated as follows:

	Total	As TiN	In Solution at 1200°C
%Ti	0.0060	0.0056	0.0004
%N	0.0060	0.0016	0.0044

The titanium is effectively all precipitated at 1200°C leaving 0.004% nitrogen in solution. According to Thelning (1980) the effective titanium content (in solution) is

$$\%Ti_{eff} = \%Ti - 5(\%N - 0.002)$$

The effective titanium content would drop to zero for a nitrogen content of 0.0032%. This would leave 0.0028% nitrogen in solution, essentially the same value as the previous calculation.

The remaining nitrogen would be expected to combine with aluminium as AlN as the temperature dropped below 1200°C, effectively removing all the remaining nitrogen from solution. This is confirmed by the low insoluble boron (i.e. BN) content of similarly processed steels (Croll, 1984). It is assumed in the remainder of the discussion that niobium, vanadium, boron and carbon are in solution in austenite at about 1050°C, and all the titanium and nitrogen have been precipitated.

At the austenitizing temperature of about 900°C, Figure 18 indicates that the vanadium would remain in solution, but niobium would be partially in solution and partially precipitated as NbC (The BIS 812 EMA sample contains 0.14% C, 0.010% Nb and 0.022% V). Depending on which solubility relation is selected, the predicted equilibrium amount of niobium in solution is 0.003% to 0.004% leaving 0.006% to 0.007% precipitated as NbC. This phase is expected to begin precipitating below about 1000°C (after hot rolling and during austenitizing). Therefore one would expect most of the vanadium to remain in solid solution together with about 0.003% niobium after quenching. This would then be available to precipitate as (Nb,V)C during tempering at 450 to 650°C.

It is clear that NbC precipitation is a borderline case for BIS 812 EMA at an austenitizing temperature of 900°C. Some factors which could further affect the partitioning of niobium between solute and precipitate include:

(i) The kinetics of NbC precipitation are slow except when there is a high dislocation density (as in controlled rolling) to act as nucleation sites (Pickering, 1984; Appendix 4).

(ii) Alloying elements such as manganese, chromium and nickel increase the solubility of titanium, niobium and vanadium carbo-nitrides (Koyama, Ishii and Narita, 1971; Table 2).

(iii) Precipitation of a carbo-nitride phase (e.g. TiN) at high temperature tends to enhance the precipitation of a less stable phase such as NbC at lower temperature (Strid and Easterling, 1985). EDS analysis of the cuboidal "TiN" precipitates in BIS 812 EMA indicates that this occurs to some extent in the present case.

Some recent papers on the modelling of alloy carbo-nitride solubility in austenite and the precipitation hardening potential of these phases include Sharma, Lakshmanan and Kirkaldy (1984), Lin and Hendrickson (1988) and Rios (1988).

The TEM observations of Section 3 show that some niobium precipitates on TiN particles formed at high temperature before or during austenitizing of BIS 812 EMA. However the hardness measurements also show that some niobium remains in solution in austenite and contributes to retardation of softening during tempering. It remains unclear whether all the niobium is accounted for by these two observations. Some niobium could also occur as extremely fine particles precipitated in the austenite. As detailed in Appendix 4, these precipitates (if present) are expected to be in the form of randomly-distributed spheroidal particles, possibly with coarser precipitates on austenite sub-grain boundaries.

The TEM observations, solubility calculations and hardness measurements during tempering all indicate that the vanadium remains in solution in BIS 812 EMA after quenching. Observations on steels with higher vanadium contents (Appendix 3) show that the vanadium precipitates on dislocations during tempering as VC or V_4C_3. The precipitates are usually in the form of thin discs on the {100} ferrite planes. Similar precipitation would be expected in BIS 812 EMA, but it must be on too fine a scale to be detected using TEM. The same considerations apply to the niobium retained in solution on quenching.

In the discussion to date, the precipitation of titanium, niobium and vanadium have been considered as distinct processes. However, it is clear from experimental and theoretical studies that the different microalloying elements interact and in fact precipitate as particles of mixed (Ti, Nb, V) (C, N) composition. Strid and Easterling (1985) and Speer, Michael and Hanssen (1987) developed models predicting the composition and volume fraction of alloy carbo-nitrides in austenite as functions of steel composition and temperature.

The latter authors also experimentally determined precipitate compositions in a steel similar to BIS 812 EMA but lower in carbon and higher in niobium and vanadium (0.09% C, 2.0% Mn, 0.027% Al, 0.015% N, 0.030% Nb, 0.051% V, < 0.002% Ti). On holding at 954°C after hot rolling, matrix precipitates grew from an initial size of 2 to 4 nm to about 50 nm after three hours. The niobium:vanadium ratio in the precipitates was about 85:15, and about 65:35 for the coarser austenite grain boundary precipitates. The Nb:V ratio increased for higher hold temperature and decreased at lower temperature (as expected from the relative solubility of niobium and vanadium carbo-nitrides). Emenike and

Billington (1989) and Lehtinen and Hansson (1989) have also examined mixed carbide precipitation in multiply microalloyed HSLA steels.

For BIS 812 EMA it is therefore possible that a small proportion of the vanadium could occur with niobium carbide precipitated in the austenite. It is probable that niobium and vanadium precipitate together as (Nb, V)C during tempering.

5. Summary

The main observations of this investigation may be summarised as follows. The microstructure of BIS 812 EMA in its usual quenched and tempered condition consists of:

(i) Tempered lath martensite typical of alloy steels of this carbon content.

(ii) Globular (with aspect ratios up to about 3:1) cementite particles, mostly on martensite lath and prior austenite grain boundaries, formed during tempering.

(iii) Widmanstatten cementite particles, within coarse martensite laths, formed during the quench.

(iv) Cuboidal TiN precipitates about 10 to 100 nm in size formed at high temperature on cooling after casting. Some niobium is associated with these precipitates and with similar coarse (several microns) inclusions formed during casting.

No other niobium or vanadium precipitates were detected using TEM. However calculations indicate that all of the vanadium and some of the niobium are in solution at the austenitizing temperature. The niobium and vanadium dissolved in austenite retard softening during tempering (confirmed using hardness testing of laboratory-produced steels without niobium and without niobium or vanadium). The (Nb, V)C precipitates formed during tempering are too fine to be detected using TEM.

6. References

Akselsen, O.M., Grong, O. and Kvaale, P.E. (1986).
A comparative study of the HAZ properties of B-containing low alloy steels. *Metallurgical Transactions A*, **17A**, 1529.

Ashby, M.F. and Easterling, K.E. (1982).
A first report on diagrams for grain growth in welds. *Acta Metallurgica*, **30**, 1969–1978.

ASM (1978).
ASM Metals handbook, 9th edition, Vol. 1, p. 196. Metals Park: American Society for Metals.

Bain, E.C. and Paxton, H.W. (1966).
Alloying elements in steel, 2nd edition. Metals Park: American Society for Metals.

Baker, T.N. (1978).
Microalloyed steels. *Science Progress*, **65**, 493–542.

Cameron, T.B. and Morral, J.E. (1986).
The solubility of boron in iron. *Metallurgical Transactions A*, **17A**, 1481–1483.

Chen, Z., Loretto, M.H. and Cochrane, R.C. (1987).
Nature of large precipitates in Ti-containing HSLA steels. *Materials Science and Technology*, **3**, 836–844.

Coladas, R., Masounave, J. and Bailon, J.-P. (1977).
The influence of Nb on the austenite processing of medium and high carbon steels. In *The Hot Deformation of Austenite*, ed. J.H. Ballance, p. 341–377. New York: TMS-AIME.

Croll, J.E. (1984).
Production and usage of quenched and tempered steel plate in Australia. In *HSLA Steels*, ed. D.P. Dunne and T. Chandra, University of Wollongong, p. 247.

Crowther, D.N. and Mintz, B. (1986).
Influence of grain size and precipitation on hot ductility of microalloyed steels. *Materials Science and Technology*, **2**, 1099–1105.

Crowther, D.N., Mohamed, Z. and Mintz, B. (1987).
The relative influence of dynamic and static precipitation on the hot ductility of microalloyed steels. *Metallurgical Transactions A*, **18A**, 1929.

Davenport, A.T., Miner, R.E. and Kot, R.A. (1977).
The recrystallisation of austenite during the hot rolling of a Nb-bearing HSLA steel. In *The Hot Deformation of Austenite*, ed. J.H. Ballance, p. 186–203. New York: TMS-AIME.

Dutta, B. and Sellars, C.M. (1986).
Strengthening of austenite by niobium during hot rolling of microalloyed steel. *Materials Science and Technology*, **2**, 146.

Dutta, B. and Sellars, C.M. (1987).
Effect of composition and process variables on Nb(C,N) precipitation in Nb microalloyed austenite. *Materials Science and Technology*, **3**, 197–206.

Edmonds, D.V. and Honeycombe, R.W.K. (1978).
Precipitation in iron base alloys. In *Precipitation Processes in Solids*, ed. K.C. Russel and H.I. Aaronson. Warrendale: TMS-AIME.

Emenike, C.O.I. and Billington, J.C. (1989).
Formation of precipitates in multiple microalloyed pipeline steels. *Materials Science and Technology*, **5**, 566–574.

Feng, B., Chandra, T. and Dunne, D.P. (1989).
Effects of alloy nitride particle size distribution on austenite grain coarsening in Ti- and Ti-Nb- bearing HSLA steels. *Materials Forum*, **13**, 139–146.

Hoogendorn, T.M. and Spanraft, M.J. (1977).
Quantifying the effect of microalloying elements on structures during processing. In *Micro Alloying 75*, p. 75–85. New York: Union Carbide.

Honeycombe, R.W.K. (1981).
Steels - microstructure and properties. London: Edward Arnold.

Irani, J.J., Burton, D. and Keyworth, F. (1966).
Quenched and tempered low carbon steels containing niobium or vanadium. *Journal of the Iron and Steel Institute*, **204**, 702–710.

Irvine, J. and Baker, T.N. (1979).
Effect of rolling deformation on niobium carbide particle size distribution in low carbon steel. *Metal Science*, **13**, 228–237.

Jonas, J.J. and Weiss, I. (1979).
Effect of precipitation on recrystallisation in microalloyed steels. *Metal Science*, **13**, 238–245.

Kampschaefer, G.W. and Jesseman, R.J. (1977).
Use of microalloyed steels in heavy construction. In *Micro Alloying 75*, p. 694–707. New York: Union Carbide.

Kestenbach, H.-J., Rodrigues, J.A. and Dermonde, J.R. (1989).
Niobium carbonitride precipitation in low carbon high manganese steel after hot rolling. *Materials Science and Technology*, **5**, 29–35.

Killmore, C.R., Harris, G.R. and Williams, J.G. (1984).
Titanium-treated C-Mn, C-Mn-Nb and C-Mn-V heavy structural plate steels with improved toughness. In *HSLA Steels*, ed. D.P. Dunne and T. Chandra, University of Wollongong, p. 57.

Koyama, S., Ishii, T. and Narita, K. (1971).
Effect of Mn, Si, Cr and Ni on the solubility and precipitation of Nb carbide in iron austenite. *Journal of the Japanese Institute of Metals*, **35**, 1089–1094.

Law, N.C., Howell, P.R. and Edmonds, D.V. (1979).
Structure of lath martensite and occurrence of retained austenite in as-quenched Fe-V-C low alloy steels. *Metals Science Journal*, **13**, 507–515.

Lehtinen, B. and Hansson, P. (1989).
Characterisation of microalloy precipitates in HSLA steels subjected to different weld thermal cycles. *Scandinavian Journal of Metallurgy*, **18**, 295–300.

Leslie, W.C. (1981).
The physical metallurgy of steels. New York: McGraw Hill.

Lin, H.-R. and Cheng, G.-H. (1987).
Hardenability effect of boron on carbon steels. *Materials Science and Technology*, **3**, 855–859.

Lin, H.-R. and Hendrickson, A.A. (1988).
The prediction of precipitation strengthening in microalloyed steels. *Metallurgical Transactions A*, **19A**, 1471–1480.

Liu, W.J. and Jonas, J.J. (1988).
A stress relaxation method for following carbonitride precipitation in austenite at hot working temperatures. *Metallurgical Transactions A*, **19A**, 1403–1414.

Llewelyn, D.T. and Coo. ٧.T. (1974).
Metallurgy of boron-treated low alloy steels. *Metals Technology*, **1**, 517.

Locci, I.E. and Michal, G.M. (1989).
The influence of annealing in the ferrite plus austenite phase field on the stability of vanadium carbide precipitates. *Metallurgical Transactions A*, **20A**, 237.

Lubuska, A.Z. (1977).
Use of microalloyed steels in shipbuilding. In *Micro Alloying 75*, p. 724–735. New York: Union Carbide (Washington Conference, 1975).

Manganon, P.L. and Heitmann, W.E. (1977).
Subgrain and precipitation-strengthening effects in hot-rolled columbium-bearing steels. In *Micro Alloying 75*, p. 59–70. New York: Union Carbide.

Matsuda, S. and Okumura, N. (1978).
Effect of distribution of Ti nitride precipitate particles on the austenite grain size of low carbon and low alloy steels. *Transactions of the Iron and Steel Institute of Japan*, **18**, 198–205.

McLean, A. and Kay, D.A.R. (1977).
Control of inclusions in HSLA steels. In *Micro Alloying 75*, p. 215–230. New York: Union Carbide.

Melloy, G.F., Slimmon, P.R. and Podgursky, P.P. (1973).
Optimizing the boron effect. *Metallurgical Transactions*, **4**, 2279.

Meyer, L., Heisterkamp, F. and Mueschenborn (1977).
Cb, Ti and V in normalised thermo-mechanically treated and cold-rolled steels. In *Micro Alloying 75*, p. 153–167. New York: Union Carbide.

Nakasato, F. and Ohtani, H. (1983).
Notch toughness of boron-treated high strength structural steels. *Metals Technology*, **10**, 333.

Ouchi, C., Sanpei, T., Okita, T. and Kozasu, I. (1977).
Microstructural changes of austenite during hot rolling and their effects on transformation kinetics. In *The Hot Deformation of Austenite*, ed. J.H. Ballance, p. 316–340. New York: TMS-AIME.

Petty, E.R. (1970).
Martensite — Fundamentals and technology. London: Longman.

Pickering, F.B. (1977).
HSLA Steels — A decade of progress. In *Micro Alloying 75*, p. 9–30. New York: Union Carbide.

Pickering, F.B. (1984).
The spectrum of microalloyed HSLA steels. In *HSLA Steels — Technology and Applications*, p. 1–31. Metals Park: American Society for Metals (Philadelphia Conference, 1983).

Pienaar, G. (1986).
Effects of V on the upper nose temper embrittlement and other mechanical properties of Cr-Ni-Mo low alloy steels. *Materials Science and Technology*, **2**, 1051–1061.

Rios, P.R. (1988).
Expression for solubility product of niobium carbonitride in austenite. *Materials Science and Technology*, **4**, 324.

Roberts, W. (1984).
Recent innovations in alloy design and processing of microalloyed steels. In *HSLA Steels — Technology and Applications*, p. 33–65. Metals Park: American Society for Metals.

Sellars, C.M. and Beynon, J.H. (1984).
Microstructural development during hot rolling of titanium microalloyed steels. In *HSLA Steels*, ed. D.P. Dunne and T. Chandra, University of Wollongong, p. 142.

Shams, N. (1986).
Carbonitride precipitates in HSLA steels. *Journal of Metals*, **38**, 31.

Sharma, R.C., Lakshmanan, V.K. and Kirkaldy, J.S. (1984).
Solubility of Nb carbide and Nb carbonitride in alloyed austenite and ferrite. *Metallurgical Transactions A*, **15A**, 545–553.

Siebert, C.A., Doane, D.V. and Breen, D.H. (1977).
The hardenability of steels, p. 115 ff. Metals Park: American Society for Metals.

Siwecki, T., Sandberg, A. and Roberts, W. (1984).
Processing characteristics and properties of Ti-V-N steels. In *HSLA Steels — Technology and Applications*, p. 619–634. Metals Park: American Society for Metals.

Speer, J.G., Michael, J.R. and Hansen, S.S. (1987).
Carbonitride precipitation in Nb/V microalloyed steels. *Metallurgical Transactions A*, **18A**, 211–222.

Speer, J.G., and Hansen, S.S. (1989).
Austenite recrystallisation and carbonitride precipitation in niobium microalloyed steels. *Metallurgical Transactions A*, **20A**, 25–38.

Stark, P.O. (1987).
A new generation of extra high strength steel for submarine pressure hulls. In *Fabrication and Inspection of Submarine Pressure Hulls*, ed. J.R. Matthews, DREA, Dartmouth, N.S., May 1987.

Strid, J. and Easterling, K.E. (1985).
On the chemistry and stability of complex carbides and nitrides in microalloyed steels. *Acta Metallurgica*, **33**, 2057–2074.

Sugimoto, K., Sakaki, T., Miyagawa, O. and Horie, T. (1986).
Effects of B and N on fracture toughness of B-treated 0.35% carbon steels tempered at low temperature. *Transactions of the Iron and Steel Institute of Japan*, **26**, 328.

Tekin, E. and Kelly, P.M. (1965).
Secondary hardening of vanadium steels. *Journal of the Iron and Steel Institute*, **203**, 715–720.

Thelning, K.-E. (1980).
In *Boron in steels*, ed. S.K. Banerji and J.E. Morral, p. 127–146. Warrendale: TMS-AIME.

Thomas, G. and Chen, Y.-L. (1981).
Structure and mechanical properties of Fe-Cr-Mo-C alloys with and without boron. *Metallurgical Transactions A*, **12A**, 933.

Vlasov, N.N. (1977).
Microalloying of carbon steels with V and Co. In *Micro Alloying 75*, p. 188–192. New York: Union Carbide.

Watanabe, S. and Ohtani, H. (1983).
Precipitation behaviour of boron in high strength steel. *Transactions of the iron and steel institute of Japan*, **23**, 38.

Weiss, I. and Jonas, J.J. (1979).
Interaction between recrystallisation and precipitation during the high temperature deformation of HSLA steels. *Metallurgical Transactions A*, **10A**, 831–840.

Wilcox, J.R. and Honeycombe, R.W.K. (1987).
Effect of precipitation on hot ductility of Nb and Al microalloyed steels. *Materials Science and Technology*, **3**, 839–854.

Wilkes, P. (1968).
Ti microalloyed hot rolled strip steels — Production properties and applications. In *HSLA Steels — Technology and Applications*, p. 33–65. Metals Park: American Society for Metals.

Wilson, A.D. (1984).
Characterising inclusion shape control in low-sulphur C-Mn-Nb steels. In *HSLA Steels — Technology and Applications*, p. 419. Metals Park: American Society for metals.

Yuoyi, C. and Xinlai, H. (1984).
A study of austenite grain boundary segregation of boron and its effect on the hardenability of steel. In *HSLA Steels*, ed. D.P. Dunne and T. Chandra, University of Wollongong, p. 327.

Appendix 1

Effect of Boron on Hardenability

The effect of boron on the hardenability of alloy steels has been reviewed by Llewelyn and Cook (1974) and Siebert, Doane and Breen (1977) and the following discussion is largely based on their conclusions. Boron increases hardenability only when in solution in austenite. Therefore, additions of about 0.03% Al and 0.03% Ti (or other nitride-former) to the steel are necessary to "protect" the boron, ensuring that it is present in soluble form rather than as oxide or nitride. An expression for the effective (soluble) boron content is:

$$\%B_{eff} = \%B - [(\%N - 0.002) - \%Ti/5 - \%Zr/15]$$

The maximum hardenability effect occurs at a soluble boron content of about 0.001% (10 ppm) and decreases again for larger boron additions. The maximum solubility in both ferritic and austenitic iron is of the order of 0.002% (Cameron and Morral, 1986).

The degree of hardenability conferred by boron is controlled by several factors including:

(i) Carbon content
(ii) Austenitizing time and temperature
(iii) Total and soluble boron content

The improvement in hardenability due to boron decreases as the carbon content increases. Two expressions (Siebert *et al.* 1977) for the boron multiplying factor for calculating ideal diameter (D_I) are:

$$f_B = 1 + 2.7\ (0.85 - \%C)$$
$$f_B = 1 + 1.76\ (0.74 - \%C)$$

The austenitizing temperature and time are important because they determine the extent to which boron and other nitride-forming elements (such as Al, Ti, Nb and V) are in solution. They also control the degree of segregation of (soluble) boron to austenite grain boundaries. It appears that it is necessary for boron to be segregated to the austenite grain boundaries (in addition to being in solution) in order to improve hardenability. High austenitizing temperatures (> 1000°C) cause "boron fade" (loss of hardenability effect) due to either or both of the following mechanisms:

(i) Dispersal of grain boundary segregation of boron.

(ii) Degradation of the protection offered by nitride-forming alloy additions. At high temperatures the alloy nitrides dissolve, and during quenching (especially of thick sections), boron is removed from solution as BN or other precipitate due to the high diffusivity of boron compared with Ti or Al.

Depending on the extent of boron precipitate formation, the hardenability can be restored by holding at a lower austenitizing temperature before quenching. This allows soluble boron to again segregate to austenite grain boundaries.

Total boron content in excess of the optimum 0.001% in solution decreases hardenability (and toughness) because the excess occurs as a precipitate network on the austenite grain boundaries. The precipitates have been variously identified as BN, $Fe_{23}(C,B)_6$ and Fe_2B, or simply as the "boron constituent". Precipitation of boron-containing phases follows conventional C-curve kinetics with the nose at about 700 to 850°C. Boron has little effect on the tempering characteristics of quenched steels apart from further precipitation of boron constituent.

The addition of boron at BHP Slab and Plate Products Division to steels similar to BIS 812 EMA has been described by Croll (1984). Optimum boron levels are stated as 0.001 to 0.002% in soluble form, and for this mill insoluble boron content is almost always less than 0.0005% (half the plates have less than 0.0001% insoluble boron).

The effect of boron on steels of similar composition to BIS 812 EMA has been investigated by Melloy, Slimmon and Podgursky (1973) and by Watanabe and Ohtani (1983). The latter authors studied a steel containing B, Al and V but no Ti or Nb. An austenitizing temperature of 1100°C was insufficient to dissolve AlN. However, at 1300°C the Al, B and N were in solution, and precipitation of BN or $Fe_{23}(C,B)_6$ on the austenite grain boundaries was generally favoured over AlN precipitation during cooling or on tempering after quenching from 1300°C.

Melloy *et al.* (1973) studied twelve similar steels treated with both Al and Ti, and containing boron ranging from 0.0001% to 0.0110%. They found an optimum (total) boron content of 0.0015 to 0.0025%. They also observed that a boron constituent (Fe_2B) formed on austenite grain boundaries on cooling from high austenitizing temperatures. The amount of this phase increased as the amount of boron was increased (becoming significant for more than about 0.0040% boron). If the steel were quenched, fine austenite grain boundary precipitation of $Fe_{23}(C,B)_6$ occurred instead of Fe_2B. Loss of hardenability at high boron contents was attributed to nucleation of ferrite by the grain boundary precipitates.

Some other recent studies of the effect of boron include Thomas and Chen (1981), Nakasato and Ohtani (1983), Youyi and Xinlai (1984), Akselsen, Grong and Kvaale (1986), and Sugimoto *et al.* (1986). Lin and Cheng (1987) used a slightly modified form of the expression for the effective boron content:

$$\%B_{eff} = \%B - (11/14)[\%N - (14/48)\%Ti]$$

and found that $\%B_{eff}$ must exceed zero in order to ensure a boron hardenability multiplying factor in excess of two.

Appendix 2

Precipitation of Titanium

Of the microalloying additions made to steel, titanium is frequently the first to precipitate after casting because it forms a range of very stable compounds (sulphides, oxides, nitrides). For this reason titanium often occurs in coarse non-metallic inclusions. Deoxidation practice and the sequence in which additions are made can have an important effect on the final distribution of microalloys.

The most stable titanium compound is TiO_2, and unless the steel is fully killed with Al, titanium occurs as TiO_2 particles in the steel (Sellars and Beynon, 1984). In the case of Al-killed steels, the destinations of microalloy titanium (Roberts, 1984; Williams, 1984) are as follows:

(i) Some titanium precipitates with manganese as (Mn,Ti)S during the final stages of solidification.

(ii) The next phase to form is TiN, with a particle size of about 15 μm when precipitated from the melt or about 1 μm when precipitated at high temperature in the solidified ingot or slab. TiN continues to precipitate as the temperature falls and solubility decreases (see below).

(iii) TiC precipitates at lower temperature in austenite or ferrite if the titanium concentration is in excess of the Ti:N stoichiometric ratio (i.e. if titanium remains in solution when all the N is consumed as TiN). Williams (1984) gives the following expressions for the amount of titanium available for TiC precipitation:

$$\%Ti_{eff} = \%Ti - (48/14)\%N - (48/32)\%S \quad (\text{for } \%Mn < 0.40)$$
$$\%Ti_{eff} = \%Ti - (48/14)\%N \quad (\text{for } \%Mn > 1.00)$$

Niobium and vanadium form carbides and nitrides like titanium but do not have the same propensity to combine with oxygen and sulphur (Meyer et al., 1977; Shams, 1986). The solubilities of their carbo-nitrides are higher than that of titanium carbo-nitride. Therefore niobium and vanadium are less likely to be found in coarse precipitates and inclusions than titanium.

Returning to the question of TiN precipitation in austenite after casting, there have been numerous studies on steels microalloyed with titanium. Roberts (1984) examined a steel with 0.011% Ti, 0.048% V and 0.008% N cast both as ten tonne ingots and as 220 mm (continuous cast) slab. For this composition, the titanium solubility limit is exceeded when the temperature falls below about 1300°C. The TiN precipitates which begin to form below this temperature have a characteristic cuboidal shape and reach a size of about 8 nm (cube edge dimension) in concast slab and about 60 nm in ingots due to the slower cooling rate. The precipitates are very stable and show only a small amount of Ostwald ripening during soaking and hot rolling. The precipitates are not effective for precipitation hardening but do reduce impact toughness and restrain grain growth in the austenite.

Similar results were obtained by Killmore *et al.* (1984) and Feng *et al.* (1989) for microalloyed steel produced by BHP Slab and Plate Products Division. For a steel with 0.14% C, 1.0% Mn, 0.03% Al, 0.015% Ti and 0.005% N cast as 220 mm slab, the TiN cuboids have a modal size of 10 nm, with most less than 30 nm. Particle density is about 10^7 per mm^2 (from TEM replicas). For a steel with 0.13% C, 1.45% Mn, 0.03% Al, 0.016% Ti and 0.006% N the modal size of the particles at various stages of processing reported by Feng *et al.* (1989) are as follows:

As-cast slab:	13 nm
Slab reheated to 1250°C and quenched:	35 nm (due to dissolution of fine particles)
Slab reheated to 1250°C and air cooled:	20 nm (due to re-precipitation during slow cooling)
Commercially hot rolled plate:	19 nm

Siwecki *et al.* (1984) also observed TiN cuboids, but an unusual result of their investigation was the observation of fine, coherent, disc-shaped precipitates of TiN and V(C,N) in plate in the hot rolled condition.

The kinetics of Ti(C,N) precipitation has been investigated by Liu and Jonas (1988) using a stress relaxation technique. They mapped out precipitation C-curves for a range of titanium contents.

Appendix 3

Tempering of Quenched and Tempered Steels

Steels used in the quenched and tempered condition are initially heated in the austenite phase field (FCC structure) where the solubility of carbon and other alloying elements is high. They are then quenched to form a supersaturated solid solution of the BCC or BCT martensite phase. Martensite occurs in two basic forms depending on carbon content:

(i) Low carbon BCC lath martensite.
(ii) Higher carbon BCT twinned martensite.

During tempering the supersaturation is relieved by precipitation and the microstructure is further modified by recovery and recrystallisation processes. Figure A3-1 summarises the effect of tempering at various temperatures on the microstructure and hardness of (unalloyed) iron-carbon martensite (Petty, 1970; Honeycombe, 1981). The same basic processes occur for alloy steels but the alloy content has the following effects:

(i) More austenite is retained after quenching.
(ii) The tempering process is retarded.
(iii) Fine, temper resistant alloy carbides precipitate in the temperature range 450 to 650°C, replacing some of the cementite (Fe_3C) precipitated at lower temperatures.

The crystallography of phases precipitated during tempering is useful for identification purposes. A brief summary based on Petty (1970), Honeycombe (1981), Edmonds and Honeycombe (1978) and Shams (1986) follows.

Epsilon Carbide:
HCP structure with a = 0.272, c = 0.432 nm.
Narrow laths or rods on {100} matrix planes.
Pitsch-Schrader orientation relationship.

Cementite:
Orthorhombic structure with a = 0.509, b = 0.674, c = 0.452 nm.
Widmanstatten rods on {110} matrix planes.
Films on lath boundaries and prior austenite grain boundaries (which later spheroidise).
Plates on {112} twin boundaries.
Bagaryatski orientation relation (all three forms).

Ti, Nb, V Carbo-Nitrides:
NaCl structure with a = 0.41 to 0.46 nm.
Plates on {100} planes, nucleated on dislocations, cementite particles or lath or grain boundaries.
Baker-Nutting orientation relation.
(When precipitated from austenite the carbo-nitrides often occur as cuboids with cube-cube orientation relation).

Chromium:
Occurs as $(Fe, Cr)_3C$, Cr_7C_3 or $Cr_{23}C_6$

Molybdenum and Tungsten:
Occur as M_2C or M_6C for high alloy content or as $(Fe, M)_3C$ or $M_{23}C_6$ for lower levels.

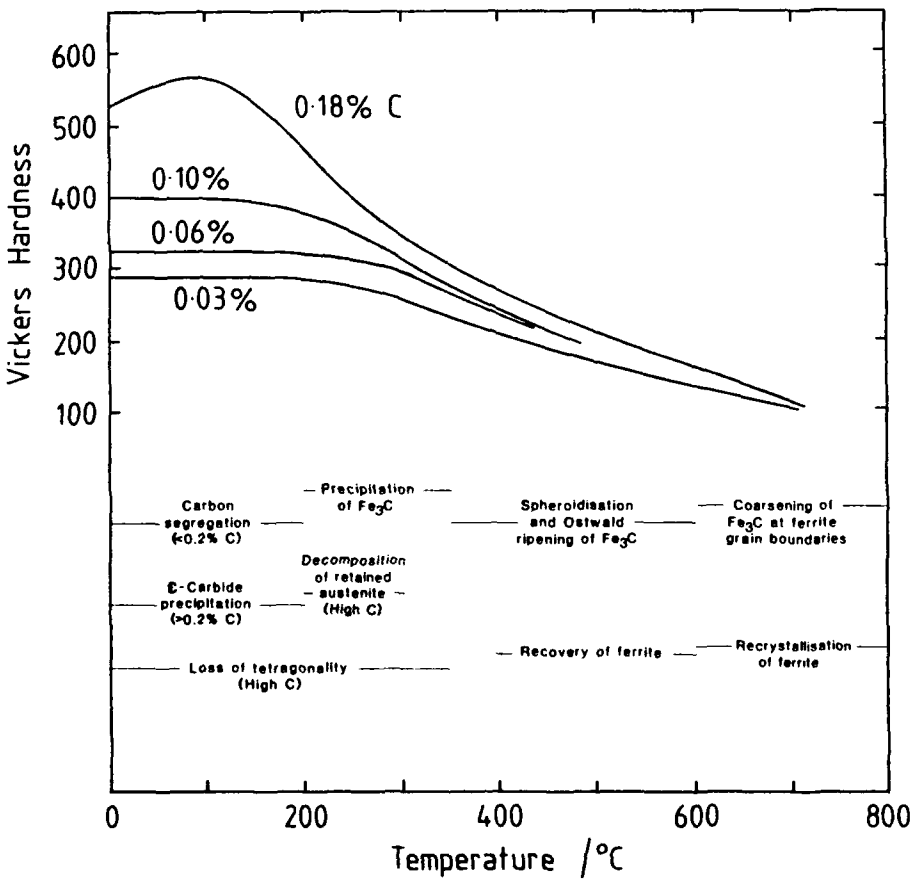

Figure A3-1: Summary of the change in hardness and microstructure during tempering of carbon steels with various carbon contents (tempering time equals one hour at the temperatures shown).

In the case of BIS 812 EMA, the content of Cr and Mo is sufficiently low that they are unlikely to occur as distinct carbides. Instead they are expected to be found with Fe as cementite. Vanadium is also soluble in cementite (Pickering, 1984).

Most studies of the tempering of steels have been concerned with alloy constructional steels and tool steels, with higher carbon and alloy content than steels of current interest. The small amount of information on quenched and tempered microalloyed steels has been reviewed by Baker (1978) and Pickering (1984). For these steels interest centres on the precipitation of Ti, Nb and V carbo-nitrides, and in particular on vanadium because of its high solubility in austenite. Vanadium is therefore the most likely microalloy to be available for precipitation during tempering.

Tekin and Kelly (1965) used electron microscopy to examine 0.1% C, 0.5%V and 0.2% C, 1.0% V steels quenched from 1000°C and tempered. They found that the vanadium addition retards recovery and postpones the dissolution of Widmanstatten cementite up to tempering temperatures of about 500°C. For the 1% vanadium steel, vanadium carbide (V_4C_3 a = 0.417 nm) was first detected in diffraction patterns after 15 hours at 450°C, as faint dots on dislocations after about 100 hours at 500°C, and in precipitate dark field images after 50 hours at 550°C. After tempering at 650 to 700°C the vanadium carbide was found on martensite needle boundaries rather than on dislocations.

For the 0.5% vanadium steel, Tekin and Kelly observed precipitates in the form of fine discs on {100} planes after tempering for about ten hours. The precipitates nucleated on dislocations and were less than 10 nm in diameter. Electron diffraction spots due to vanadium carbide were difficult to detect.

Raynor *et al.* (1966) obtained similar results for a 0.2% C, 2.0% V alloy. Wilkes (1968) studied a 0.13% C, 1.1% V steel using electron microscopy and electrical resistivity. He observed fine scale precipitation on dislocations after tempering for five hours at 650°C. The precipitation kinetics (from resistivity) were also consistent with precipitation on dislocations.

Most studies are agreed (Baker, 1978) that vanadium carbide precipitates on dislocations, and in the matrix in the form of thin plates. At peak hardness they are 5 to 10 nm in diameter and 0.5 to 1 nm thick, and have a density of about 10^{17} per cm^3. The particles retard the tempering process by pinning dislocations and retaining them for longer times and at higher tempering temperatures.

Pienaar (1986) observed Widmanstatten V_4C_3 precipitates after tempering at 675°C a steel with 0.3% C, 0.65% Cr, 2.4% Ni, 0.5% Mo and 0.4% V. Locci and Michal (1989) obtained a fine distribution of V_4C_3 precipitates after quenching a steel with 0.14% C and 0.49% V and tempering at 700°C. Vlasov (1977) studied the effects of vanadium additions ranging from 0.01 to 0.10% to a 0.2% C steel quenched from 900°C. The vanadium had a large effect on hardness after tempering at 600°C but not at 400°C.

Few studies of the tempering of steels containing microalloy levels of vanadium (e.g. 0.03% as in BIS 812 EMA) have been reported. However it is clear from the work described above that vanadium carbide precipitation would be difficult to detect by electron microscopy in steels with such a small vanadium content, tempered for the relatively short times involved in the processing of BIS 812 EMA.

Irani, Burton and Keyworth (1966) examined a series of steels containing about 0.04% C, 1.5% Mn and either 0.05 to 0.16% vanadium or 0.02 to 0.14% niobium. After quenching from 950°C (to an acicular ferrite or bainite structure) tempering caused a secondary hardening peak for all steels in the temperature range 500 to 650°C. This was attributed to precipitation of V(C,N) or Nb(C,N) on dislocations.

However the micrographs presented in support of this claim (for a steel containing 0.16% V tempered four hours at 550°C) do not constitute convincing evidence of such precipitation.

A limited number of results are available for quenched and tempered steels containing niobium or titanium. However these elements have been shown to significantly retard dislocation rearrangement and recovery processes during tempering.

Appendix 4

Niobium Precipitation in Austenite

Introduction

The precipitation of niobium in austenite has been reported in numerous papers concerned mostly with the controlled rolling of HSLA steels. Niobium has the effect of restraining recrystallisation of austenite and therefore reducing grain size. Crowther, Mohamed and Mintz (1987) identified the following types of precipitation in austenite:

(i) Pre-existing precipitates (undissolved during the soak).
(ii) Static precipitation during continuous cooling.
(iii) Dynamic precipitation during hot rolling.
(iv) Static precipitation in a deformed matrix (after rolling).

It is well known that precipitation of Nb(C,N) and other carbonitrides is accelerated by deformation, so the final two categories are also known as strain-assisted precipitation.

Precipitate Morphology and Distribution

Crowther *et al.* studied a steel with 0.12% C, 1.4% Mn, 0.010% N and 0.034% Nb, solution treated to dissolve all precipitates and then held at 950°C (with and without deformation). They observed the precipitation of Nb(C,N) after times of 0, 2 and 6 hours at 950°C.

(i) 0 Hours: Extensive precipitation of spheroidal particles about 15 nm in size in the matrix and on austenite grain boundaries (during cooling from the soak).

(ii) 2 Hours: Bimodal particle size distribution with an average size of 25 nm.

(iii) 6 Hours: Some fine particles in the matrix, but mostly faceted spheroidal precipitates on austenite grain boundaries about 55 nm in size.

Similar results were obtained for a steel with 0.11% C and 0.05% V instead of niobium.

The observation of a bimodal particle size distribution and the preferential growth of grain boundary precipitates at the expense of the finer matrix precipitates is a common feature of investigations of this type. However, it should be noted that the niobium contents of the steels examined are usually much higher than that of BIS 812 EMA. Some examples of these investigations are as follows:

Davenport *et al.* (1977) observed extrememly fine precipitates soon after hot rolling at 870°C, and on holding at that temperature a network of spheroidal precipitates developed (0.08% C, 0.09% Nb, 0.018% Al, 0.02% N).

Ouchi *et al.* (1977) and Coladas (1977) did not observe precipitates immediately after hot rolling but found spheroidal Nb(C,N) particles 5 to 10 nm in size after holding at the hot rolling temperature.

Baker (1978) found that 20 nm spheroidal precipitates formed on austenite grain and sub grain boundaries during rolling of a steel with 0.04% C, 1.4% Mn and 0.06% Nb.

Manganon and Heitmann (1977) observed a network of 40 to 100 nm particles after holding for a unspecified time at 1010°C. Their steel contained 0.07% C, 1.05% Mn and 0.05% Nb.

Irvine and Baker (1979) found that the randomly-distributed spheroidal precipitates have a typical size of 2 to 5 nm in steels with 0.04 to 0.05% C, 1.6% Mn and 0.06 to 0.08% Nb. They also observed coarser precipitates outlining austenite sub-grain boundaries.

Crowther and Mintz (1986) examined four similar steels, one of which contained 0.12% C, 1.45% Mn, 0.015% Al, 0.010% N and 0.034% Nb (others contained C-Mn, C-Mn-Al, C-Mn-Al-V). They noted poor hot ductility due to the presence of fine Nb(C,N) dynamically-precipitated in the matrix and on the austenite grain boundaries. Wilcox and Honeycombe (1987) also examined the effect of Nb(C,N) precipitation on hot ductility. Dutta and Sellars (1986) studied the effect of precipitation on hot strength. Fine scale precipitation (2 to 3 nm) causes a large direct strength increase. Precipitation also has an indirect effect on flow stress by restraining recovery and recrystallisation.

Kinetics of Nb Precipitation in Austenite

A variety of methods have been used to investigate the rate of niobium precipitation and study the effects of composition, deformation and temperature. These include chemical extraction of precipitates, transmission electron microscopy, secondary hardening potential, resistivity and hot deformation testing. The precipitation of Nb(C,N) follows conventional C-curve kinetics with the nose at a temperature of 900 to 1000°C and precipitation start times of the order of one minute.

Dutta and Sellars (1987) used nucleation theory and the Nb(C,N) solubility product to calculate C-curves for the commencement of precipitation, and the effect of composition and strain on the position of the curve. They obtained good agreement with the experimental observations of several authors. Their work serves as a good review of the literature on the precipitation-start C-curve but is not concerned with the further progress of precipitation. However, the interaction of precipitation and recrystallisation (see below) is considered.

Weiss and Jones (1979) used hot deformation flow curves to study Nb(C,N) precipitation kinetics (and interaction with recrystallisation) in a steel with 0.05% C, 0.04% Mn, 0.004% N and 0.035% Nb. The [Nb][C] product is similar to that of BIS 812 EMA, so similar precipitation kinetics would be expected. Some of their results are shown in Figure A4-1. At temperatures of 900 to 950°C, the approximate precipitate-start, P_s, and -finish, P_f, times for static precipitation are as follows:

(i) Undeformed austenite: P_s = 2-5 min P_f = 10-100 h
(ii) 5% Prestrain: P_s = 10-30 s P_f = 3-10 h

Dynamic precipitation occurs at a much faster rate. Jonas and Weiss (1979) observed almost identical kinetics for a steel with 0.06% C and 0.018% Nb.

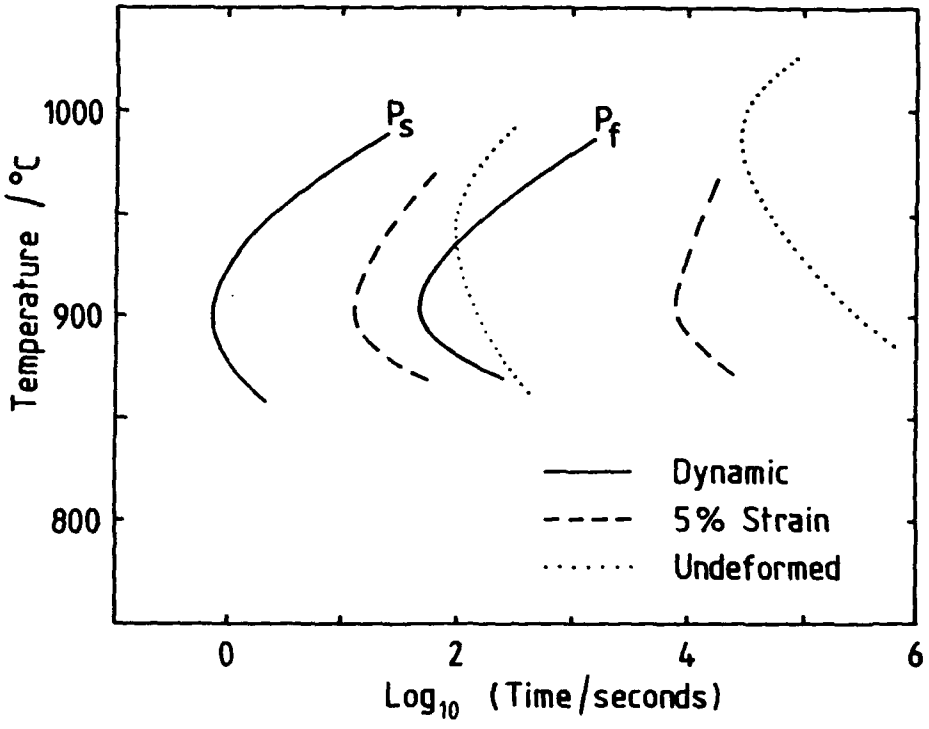

Figure A4-1: Kinetics of NbC precipitation in a steel with [Nb][C] product similar to BIS 812 EMA. Dynamic precipitation (during deformation) is very fast, and the rate of precipitation is also accelerated by prior deformation at higher temperature (from Weiss and Jonas, 1979).

Crowther *et al.* (1987) used loss of secondary hardening potential to show that Nb(C,N) precipitation at 950°C was complete in about 2.5 hours for a steel with 0.12% C, 1.4% Mn, 0.010% N and 0.034% Nb.

The work of Kestenbach, Rodrigues and Dermonde (1989) on low carbon, high niobium steels confirms the importance of deformation in accelerating Nb(C,N) precipitation during hot rolling. Very little precipitation was observed under conditions favouring the rapid recrystallisation of austenite.

Effect of Nb on Austenite Recrystallisation

The recrystallization of austenite during hot rolling is greatly retarded by niobium. It is generally assumed that this is caused by the strain-assisted precipitation of Nb(C,N) on dislocations and sub-grain boundaries. However, some investigators argue that solute drag on dislocations due to niobium in solution is more important. Speer and Hansen (1989) attempted to resolve this problem by examining a series of steels with:

(a) Constant Nb(C,N) supersaturation, but variable Nb and C contents.
(b) Constant Nb content (0.05%).

Their results show that Nb(C,N) precipitation is much more effective in retarding recrystallisation than is niobium in solution. They also studied other aspects of the interaction between Nb(C,N) precipitation and recrystallisation kinetics.

SECURITY CLASSIFICATION OF THIS PAGE **UNCLASSIFIED**

DOCUMENT CONTROL DATA SHEET

REPORT NO.	AR NO.	REPORT SECURITY CLASSIFICATION
MRL-TR-91-35	AR-006-828	Unclassified

TITLE

Electron microscope study of the microstructure of BIS 812 EMA submarine hull steel

AUTHOR(S)
I.M. Robertson

CORPORATE AUTHOR
DSTO Materials Research Laboratory
PO Box 50
Ascot Vale Victoria 3032

REPORT DATE	TASK NO.	SPONSOR
December, 1992		

FILE NO.	REFERENCES	PAGES
G6/4/8-4008	70	51

CLASSIFICATION/LIMITATION REVIEW DATE

CLASSIFICATION/RELEASE AUTHORITY
Chief, Ship Structures and Materials Division

SECONDARY DISTRIBUTION

Approved for public release

ANNOUNCEMENT

Announcement of this report is unlimited

KEYWORDS

Carbo-nitride inclusions
Inclusions
Austenite
Tempering
Quenching

ABSTRACT

The hull steel for Australia's Collins class submarine, BIS 812 EMA, is somewhat unusual in that it contains significant additions of boron and the substitutional hardenability elements nickel, chromium and molybdenum, and is also microalloyed with titanium, niobium and vanadium. It is used in the quenched and tempered condition, rather than being control-rolled, and therefore the role and benefit conferred by the microalloying additions are not clear. The electron microscope study reported here is concerned with characterizing the microstructure of the steel and determining the distribution of the titanium, niobium and vanadium.

The steel consists of tempered lath martensite typical of quenched and tempered steels of similar carbon content. The titanium occurs as cuboidal particles, ten to one hundred nanometres in size (probably TiN), formed after solidification or during the soak, and largely unaffected by subsequent processing. The niobium and vanadium appear to be mostly taken into solution during the austenitizing treatment and precipitate as a fine carbide dispersion during tempering, although some niobium is incorporated in the "TiN" cuboids.

Electron Microscope Study of the Microstructure of
BIS 812 EMA Submarine Hull Steel

I.M. Robertson

(MRL-TR-91-35)

DISTRIBUTION LIST

Director, MRL
Chief, Ship Structures and Materials Division
Dr J.C. Ritter
Dr I.M. Robertson
MRL Information Service

Chief Defence Scientist (for CDS, FASSP, ASSCM) (1 copy only)
Director, Surveillance Research Laboratory
Director (for Library), Aeronautical Research Laboratory
Director, Electronics Research Laboratory
Head, Information Centre, Defence Intelligence Organisation
OIC Technical Reports Centre, Defence Central Library
Officer in Charge, Document Exchange Centre (8 copies)
Army Scientific Adviser, Russell Offices
Air Force Scientific Adviser, Russell Offices
Navy Scientific Adviser, Russell Offices - data sheet only
Scientific Adviser, Defence Central
Director-General Force Development (Land)
Senior Librarian, Main Library DSTOS
Librarian, MRL Sydney
Librarian, H Block
UK/USA/CAN ABCA Armies Standardisation Rep. c/- DGAT (8 copies)
Librarian, Australian Defence Force Academy
Counsellor, Defence Science, Embassy of Australia - data sheet only
Counsellor, Defence Science, Australian High Commission - data sheet only
Scientific Adviser to DSTC, C/- Defence Adviser - data sheet only
Scientific Adviser to MRDC, C/- Defence Attache - data sheet only
Head of Staff, British Defence Research and Supply Staff (Australia)
NASA Senior Scientific Representative in Australia
INSPEC: Acquisitions Section Institution of Electrical Engineers
Head Librarian, Australian Nuclear Science and Technology Organisation
Senior Librarian, Hargrave Library, Monash University
Library - Exchange Desk, National Institute of Standards and Technology, US
Exchange Section, British Library Document Supply Centre
Periodicals Recording Section, Science Reference and Information Service, UK
Library, Chemical Abstracts Reference Service
Engineering Societies Library, US
Documents Librarian, The Center for Research Libraries, US